R. & M. No. 3327

MINISTRY OF AVIATION

AERONAUTICAL RESEARCH COUNCIL
REPORTS AND MEMORANDA

Simplified Loading Formulae for Pull-Out Manoeuvres of Tailed Aeroplanes

By S. NEUMARK, Techn.Sc.D., F.R.Ae.S.

LONDON: HER MAJESTY'S STATIONERY OFFICE
1963
PRICE £1 1s. 0d. NET

Simplified Loading Formulae for Pull-Out Manoeuvres of Tailed Aeroplanes

By S. NEUMARK, Techn.Sc.D., F.R.Ae.S.

COMMUNICATED BY THE DEPUTY CONTROLLER AIRCRAFT (RESEARCH AND DEVELOPMENT), MINISTRY OF AVIATION

*Reports and Memoranda No. 3327**
June, 1958

Summary.

A method, alternative to that in common use at present, of calculating the response quantities in pull-out manoeuvres relevant to important cases of loads and stresses in aeroplane structures, is presented. The method, based on 'trapezoidal' elevator input, leads to final solutions in the form of closed formulae, which are not only convenient from the computational point of view, but which also permit a comprehensive discussion. It may be used at every stage of design, including the earliest estimates. An important part in all this work is played by 'overshoot factors', and complete charts of these are included.

The method can be easily extended to cover asymmetrical manoeuvres.

LIST OF CONTENTS

* Replaces R.A.E. Report No. Aero. 2608—A.R.C. 20,666.

LIST OF APPENDICES

LIST OF ILLUSTRATIONS

---

1. *Introduction.*

The problem of determining incremental and maximum loads in symmetric and asymmetric manoeuvres has attracted much attention in the past, and has provided the subject for a great volume of literature[1, 5 to 15]. The method normally used in Britain is that proposed by T. Czaykowski (*see* Ref. 1, where many earlier reports are referred to, and also Ref. 11).

The method of Ref. 1 consists in assuming the basic 'exponential' law, with one arbitrary parameter (k), for the elevator input. The value of the parameter is immaterial for the development of theory but has, of course, a great importance for the practical design calculations and requirements. An empirical formula for the value of k {*see* (3.19)}, explained in Ref. 1, was chosen in such a way as to obtain the best correlation between the mean elevator rate defined for the exponential input {*see* (3.16)} and that obtained from the experimental input curves for a number of most rapid manoeuvres selected from the many collected in U.S.A. up to 1950. The proposal was described in Ref. 1 as 'tentative', leaving scope for further tests to provide more information. The present method

assumes an alternative 'trapezoidal' law of elevator input (*see* Fig. 1), again with one arbitrary parameter τ_1 (or, more conveniently, $\varphi_1 = J\tau_1$ *see* Section 3.1). This assumption leads to simpler response equations, in both the aeroplane motion and wing and tail loads, so that many maxima (such as peak normal acceleration, peak tail load, etc.) can be expressed by explicit formulae, without recourse to graphical or numerical solutions of transcendental equations. As to the choice of the parameter φ_1, it is again unimportant for developing the theory (although the effects of its variation are interesting). An obvious suggestion, however, is to seek again the best correlation with experimental results.

The simple concept of trapezoidal elevator input is, of course, not new. It was used, e.g., by the early writers C. D. Perkins[6, 7] and H. A. Pearson[8], and more recently by D. R. Puttock[13, 14] (the latter applied it to the case of automatic-pilot failure). However, the analysis has never been pursued far enough, and it was thought worthwhile to push it much further, so as to obtain both a simpler presentation of all the results and a better insight into the underlying response problem.

An important feature of the analytical treatment adopted here is that maxima of the various response quantities are expressed in terms of a few overshoot factors which determine the amount by which these maxima exceed the (easily calculable) steady-state asymptotic values. The overshoots are of particular importance for tail loads because the latter consist of the negative direct contribution of elevator deflection (subject to no overshoot) and a positive contribution due to aeroplane response (this being subject to overshoot). A small error in estimating overshoot, from whatever source, may thus lead to a significant error in the resultant difference. In addition, we need to calculate many different overshoots in various flight conditions and for varying duration of the manoeuvre. The trapezoidal approach, owing to some fortunate algebraical relationships, may be manipulated into a set of a few basic overshoot factors, which it has been found easy to tabulate and chart, so that full charts are, in fact, given in the present report. It has also been possible to expand the exact formulae for overshoot factors into rapidly convergent power series leading to very simple approximations.

It will be seen in Sections 3 to 7 that the method proposed leads to peak accelerations at the c.g. and tail, and first peak incremental tail upload, which become indistinguishable from those given by Ref. 1, if the mean elevator rate is assumed the same in both cases. The peak incremental download and the second peak incremental upload for rapid manoeuvres, obtained by the method proposed under the same assumption, are appreciably larger than those from Ref. 1 so that, at least, they may be considered as conservative. Calculating design tail loads in such a way can only be recommended when this kind of conservatism is acceptable or desirable and, of course, also in all those instances where the trapezoidal type of elevator input adequately represents the actual elevator movement as, e.g. in the automatic-pilot run-away case. However, the general value of the method will have to be appraised on the basis of possible correlation with results of flight tests, and this would require considerable work far beyond the scope of this paper.

The simplifying assumptions which restrict the field covered by what follows are practically the same as those of Ref. 1, Section 3:

(1) variations of forward speed and gravity component during the disturbance are neglected,

(2) contribution of the elevator deflection to total lift is neglected,

(3) the tailplane's own pitching moment about its reference axis, due to elevator deflection, is neglected in the pitching moments' equation of the aeroplane,

(4) the elastic distortion of the structure is neglected,

(5) the equations are linearized, so that the usual first-order derivatives, supposed constant during the manoeuvre, are exclusively used, with no refinements to account for unsteady motion; it may be pointed out, however, that the aerodynamic derivatives are only considered constant for each single case (given design, fixed flight conditions), but they may and should be treated as variable with flight conditions (Mach number) even for a given design.

The restrictions (2) and (3) are usually unimportant, but can be easily removed if necessary. The restriction (1) is discussed in Section 7.3. The restrictions (4) and (5) are the only important ones, and a further development to cover elastic distortion and non-linearities is most desirable. A way is already open[16] towards the inclusion of aeroelastic effects, but it is not suggested that this can be done in a way comparable to that of the present paper, at least in the near future. It may be necessary to employ methods which, while more powerful in the computational sense, will inevitably be less efficient in the 'algebraic' sense. But, whatever different research tools may be applied, one point should never be forgotten; the value of any more elaborate studies covering elastic distortion will not only be greatly diminished but indeed often nullified if a parallel (so much simpler) computation is not simultaneously made with an assumedly rigid aeroplane. As often in similar cases, the value of numbers lies not in themselves but in comparison. Analogous remarks apply to non-linearities in the dynamic system.

No more explanation is needed here; the final discussion and conclusions are given in Sections 7 and 8. To achieve a full understanding and acquire a working ability, the reader must, of course, plough his way through Sections 2 to 5 giving the full theory, and is advised to go carefully through the numerical example of Section 6. It may be mentioned that, to obtain the final simple results, a not inconsiderable analytical effort had to be made and, to make the paper more readable, all heavy transformations and expansions have been relegated to Appendices. Analytical solutions have been obtained by using operational treatment, in the form described in Ref. 3, which contains tables of operational formulae directly applicable to response calculations.

A grateful acknowledgment is due to A. S. Taylor and to T. Czaykowski for many helpful suggestions and constructive criticism of the full report; and to Mrs. J. Collingbourne, Miss A. Dyer, Miss B. Mills and Miss F. M. Ward who have made all calculations and prepared the illustrations. Special mention is due also to D. Foster, a student of Bristol University, who, during his short stay as a vacation student at the R.A.E., contributed the laborious part summarized in Appendix IV.

2. *Basic Equations.*

Assuming no speed variation during the manoeuvres, the differential equations of motion will be written (cf. Ref. 2, App. I):

$$(D+\tfrac{1}{2}a)\hat{w} - \hat{q} = 0, \tag{2.1}$$

$$(\chi D+\omega)\hat{w} + (D+\nu)\hat{q} = -\delta\eta, \tag{2.2}$$

where $\hat{w} = \alpha$ is the incremental incidence of the main plane, $\hat{q}$ dimensionless rate of pitch, χ, ω, ν, δ concise moment derivatives, and the elevator deflection η is a prescribed function of time. The operational solutions of these equations are:

$$\hat{w} = \alpha = -\frac{\delta\eta}{D^2 + 2RD + C}, \tag{2.3}$$

$$\hat{q} = -\frac{\delta(D+\tfrac{1}{2}a)\eta}{D^2 + 2RD + C}, \tag{2.4}$$

where the denominator is the operational determinant of the system:

$$D^2 + 2RD + C = (D+R)^2 + J^2 = D^2 + (\tfrac{1}{2}a+\nu+\chi)D + (\omega+\tfrac{1}{2}a\nu), \tag{2.5}$$

R being the dimensionless damping factor and J the dimensionless frequency of the short-period oscillation. In each of the solutions, the function η should be replaced by its operational equivalent, and the formulae interpreted as functions of time, e.g. by using tables of Ref. 3.

The quantities to be investigated will be:

(i) *Coefficient of normal acceleration at c.g.* This varies in proportion to the incremental incidence $\hat{w}$:

$$n = \frac{a}{C_L}\hat{w} = -\frac{a\delta}{C_L}\frac{\eta}{D^2+2RD+C}; \tag{2.6}$$

(ii) *Effective incremental incidence of the tail* (relevant for the tail load):

$$\alpha_{\text{eff}}' = \alpha\left(1-\frac{d\epsilon}{d\alpha}\right) + \frac{lq}{V} + \frac{l}{V}\frac{d\epsilon}{d\alpha}\frac{d\alpha}{dt} = \hat{w}\left(1-\frac{d\epsilon}{d\alpha}\right) + \frac{\hat{q}}{\mu} + \frac{d\epsilon}{d\alpha}\frac{D\hat{w}}{\mu}$$

or, eliminating $\hat{q}$ by means of (2.1):

$$\alpha_{\text{eff}}' = \hat{w}\left(1-\frac{d\epsilon}{d\alpha}+\frac{a}{2\mu}\right) + \left(1+\frac{d\epsilon}{d\alpha}\right)\frac{D\hat{w}}{\mu}. \tag{2.7}$$

It is seen that the incremental incidence of the tail does not vary simply in proportion to that of the main plane ($\hat{w}$), because of the 2nd term in (2.7). It will be convenient to introduce, for abbreviation, the constant ('modifying factor for tail incidence'):

$$\lambda = \frac{J\left(1+\frac{d\epsilon}{d\alpha}\right)}{\mu\left(1-\frac{d\epsilon}{d\alpha}+\frac{a}{2\mu}\right)}, \tag{2.8}$$

which is usually small because of large values of μ, and then the formula (2.7) may be written {introducing (2.3) for $\hat{w}$}:

$$\alpha_{\text{eff}}' = -\delta\left(1-\frac{d\epsilon}{d\alpha}+\frac{a}{2\mu}\right)\frac{1+\frac{\lambda}{J}D}{D^2+2RD+C}\eta \tag{2.9}$$

(iii) *Coefficient of normal acceleration at the tail*:

This again does not vary in proportion to $\hat{w}$, being given by

$$n_t = n - \frac{l}{g}\frac{dq}{dt} = \frac{a}{C_L}\hat{w} - \frac{2}{\mu C_L}D\hat{q}$$

or, eliminating $\hat{q}$, and introducing (2.3) for $\hat{w}$:

$$n_t = -\frac{a\delta}{C_L}\frac{1-\frac{1}{\mu}D-\frac{2}{\mu a}D^2}{D^2+2RD+C}\eta. \tag{2.10}$$

In what follows, we are going to consider only manoeuvres in which the elevator is ultimately held fixed at a certain value, negative for pull-out, say $(-\eta_f)$. The quantities n, α_{eff}' and n_t will then

all tend to some 'final' (or asymptotic) values, which can be determined by neglecting all terms containing the differential operator D, and replacing η by $(-\eta_f)$. We then obtain from (2.6, 9, 10):

$$n_f = n_{t,f} = \frac{a\delta}{C_L C}\,\eta_f, \tag{2.11}$$

$$\alpha'_{\mathrm{eff},f} = \frac{\delta}{C}\left(1 - \frac{d\epsilon}{d\alpha} + \frac{a}{2\mu}\right)\eta_f, \tag{2.12}$$

and dividing the formulae (2.6, 9, 10) by their respective final values:

$$\frac{n}{n_f} = -\frac{C}{D^2 + 2RD + C}\,\frac{\eta}{\eta_f}, \tag{2.13}$$

$$\frac{\alpha'_{\mathrm{eff}}}{\alpha'_{\mathrm{eff},f}} = -\frac{C\left(1 + \frac{\lambda}{J}D\right)}{D^2 + 2RD + C}\,\frac{\eta}{\eta_f}, \tag{2.14}$$

$$\frac{n_t}{n_f} = -\frac{C\left(1 - \frac{1}{\mu}D - \frac{2}{\mu a}D^2\right)}{D^2 + 2RD + C}\,\frac{\eta}{\eta_f}. \tag{2.15}$$

The final values given in (2.11, 12) are theoretically reached only after an infinite time but in practice after only a few seconds, provided the short-period oscillation is reasonably damped. All equations are valid only under the assumption that the speed remains constant, which is the essential basis of Gates' manoeuvrability theory[4]. In reality, the motion will slowly deviate from the above simplified picture, owing to the gradually developing phugoid oscillation but, as known and as illustrated in Ref. 2, App. I, the effects during the early part of the motion, particularly as regards the important first peaks of all relevant quantities, are negligible.

It will be convenient to represent the final values (2.11, 12) in terms of the practical design data. We have:

$$\delta = -\frac{\mu m_\eta}{i_B} = \frac{\mu}{i_B}\frac{S'}{2S}\,a_2, \qquad C = \omega + \tfrac{1}{2}a\nu = \frac{\mu}{i_B}\frac{ca}{2l}\,H_m, \tag{2.16}$$

hence:

$$\frac{\delta}{C} = \frac{a_2\overline{V}}{aH_m}, \tag{2.17}$$

and thus the final values are obtained in the convenient form:

$$n_f = \frac{a_2\overline{V}}{C_L H_m}\,\eta_f, \tag{2.18}$$

$$\alpha'_{\mathrm{eff},f} = \frac{a_2\overline{V}}{aH_m}\left(1 - \frac{d\epsilon}{d\alpha} + \frac{a}{2\mu}\right)\eta_f. \tag{2.19}$$

3. *Normal Acceleration at C.G.*

3.1. *Step Elevator Input.*

In this simple case, we have $\eta = -\eta_f$ right from the start (Fig. 1), and the operational formula (2.13) becomes:

$$\frac{n}{n_f} = \frac{C}{D^2 + 2RD + C}. \tag{3.1}$$

The functional solution can be determined at once from Ref. 3 (form. 100):

$$\frac{n}{n_f} = 1 - (\cos\varphi + \beta \sin\varphi)e^{-\beta\varphi} = \Phi'(\varphi), \text{ say,} \tag{3.2}$$

where, for abbreviation:

$$\varphi = J\tau \text{ (time angle)}, \tag{3.3}$$

$$\beta = \frac{R}{J} \text{ (angular damping index)}. \tag{3.4}$$

This simple solution is well known (e.g. Ref. 1, 2) and is illustrated by the curves marked 'step input' in Figs. 2, 3, 4, for $\beta = 0,\ 0{\cdot}2,\ 0{\cdot}4$. The curves start at 0, rise to their first peak values and then oscillate, with gradually diminishing amplitude (except for $\beta = 0$), about the asymptotic value 1. The first peak value, which is the absolute maximum, is reached at $\varphi = \pi$ and is given by

$$\frac{n_{\max}}{n_f} = 1 + E_0 = 1 + e^{-\beta\pi}. \tag{3.5}$$

We shall term E_0 'overshoot factor' for the case of step input. A few numerical values are given below:

$\beta = 0$	0·1	0·2	0·3	0·4	0·5	0·6	0·8	1·0
$E_0 = 1$	0·7304	0·5335	0·3897	0·2846	0·2079	0·1518	0·0810	0·0432

and it is seen that this factor, while important for small values of β, becomes practically negligible for, say, $\beta > 1$.

3.2. *Trapezoidal Elevator Input.*

In this case, η varies linearly from 0 to $(-\eta_f)$, during the time interval τ_1, and then remains constant. During the *first part* of the manoeuvre, we have:

$$\eta = -\eta_f \frac{\tau}{\tau_1} \qquad \text{or, in operational form:} \qquad -\frac{\eta}{\eta_f} = \frac{1}{\tau_1 D} = \frac{J}{\varphi_1 D}, \tag{3.6}$$

where $\varphi_1 = J\tau_1$; the operational formula (2.13) becomes:

$$\frac{n}{n_f} = \frac{1}{\varphi_1} \frac{JC}{D(D^2 + 2RD + C)}, \tag{3.7}$$

and the functional solution will be (*see* Ref. 3, form. 111):

$$\frac{n}{n_f} = \frac{\Phi(\varphi)}{\varphi_1} = \frac{1}{\varphi_1}\left\{\varphi - \frac{2\beta}{1+\beta^2} + \left(\frac{2\beta}{1+\beta^2}\cos\varphi - \frac{1-\beta^2}{1+\beta^2}\sin\varphi\right)e^{-\beta\varphi}\right\} \qquad (\varphi < \varphi_1). \tag{3.8}$$

It may be noticed that the first derivative of the function $\Phi(\varphi)$, which is, of course, the $\Phi'(\varphi)$ of (3.2), is always positive, therefore the normal acceleration increases throughout the first part of the manoeuvre, and its first peak must occur during the second part.

For this *second part*, the elevator input may be considered as the sum of two linear inputs of opposite signs, of which the input I (Fig. 1) is proportional to τ, and input II proportional to $(\tau-\tau_1)$. The solution will therefore be:

$$\frac{n}{n_f} = \frac{\Phi(\varphi) - \Phi(\varphi-\varphi_1)}{\varphi_1} \qquad (\varphi > \varphi_1), \tag{3.9}$$

or explicitly:

$$\frac{n}{n_f} = 1 + \frac{e^{-\beta\varphi}}{\varphi_1}\left[\frac{2\beta}{1+\beta^2}\{\cos\varphi - \cos(\varphi-\varphi_1)e^{\beta\varphi_1}\} - \frac{1-\beta^2}{1+\beta^2}\{\sin\varphi - \sin(\varphi-\varphi_1)e^{\beta\varphi_1}\}\right]. \tag{3.10}$$

This represents an ordinary decaying oscillation, and the first peak will be the absolute maximum. The fact that the maximum occurs during this stage makes it possible to determine its position and value analytically. The latter is shown in Appendix I to be:

$$\frac{n_{\max}}{n_f} = 1 + E = 1 + \frac{e^{-\beta(\varphi_m-\varphi_1)}}{\varphi_1}\sqrt{\left(\frac{1 - 2e^{-\beta\varphi_1}\cos\varphi_1 + e^{-2\beta\varphi_1}}{1+\beta^2}\right)}, \tag{3.11}$$

where φ_m is the relevant value of φ, given by the formula:

$$\tan(\varphi_m-\varphi_1) = \frac{(e^{\beta\varphi_1}-\cos\varphi_1) - \beta\sin\varphi_1}{\beta(\cos\varphi_1 - e^{\beta\varphi_1}) - \sin\varphi_1} \qquad (0 < \varphi_m - \varphi_1 < \pi). \tag{3.12}$$

Several examples of the growth of the normal acceleration {according to (3.8) and (3.10)} are given in Figs. 2, 3, 4, for $\beta = 0$, $0{\cdot}2$ and $0{\cdot}4$, and for a few values of φ_1. The first peak is shown in each case. The values of the overshoot factor E are plotted, for a wide range of φ_1 and several values of β, in Fig. 5. The initial ordinates of all curves represent the overshoot factor E_0 for the case of step input {Section 3.1, form. (3.5)}. It is seen that, for $\varphi_1 > 0$, the overshoot factor is always smaller than E_0, but the curves present some peculiarities. For very small values of β, e.g. $\beta = 0{\cdot}1$, there are a few consecutive minima and maxima, at φ_1 very nearly 2π, 3π, etc. And, for $\beta = 0$, E becomes exactly 0 at $\varphi_1 = 2\pi$, 4π, etc., i.e. when the duration of the elevator movement equals the period of the aeroplane oscillations, or a multiple of this period. For larger values of β (above $0{\cdot}3$, say), as normally encountered in stable flight, E decreases monotonically as φ_1 increases.

In rapid manoeuvres, φ_1 will be quite small, certainly smaller than 2π. For practical use, a part of Fig. 5 has been shown enlarged in Fig. 6, where φ_1 varies from 0 to 2π, and β from 0 to 1. For $\beta > 1$, the overshoots may be treated as negligible.

Fig. 7 illustrates the formula (3.12) for the same range of β and φ_1 as Fig. 5. It is seen that $(\varphi_m - \varphi_1)$ initially decreases from π when φ_1 increases from 0, and afterwards oscillates about asymptotic values which are always greater than $\frac{1}{2}\pi$.

The exact formulae (3.11, 12) are somewhat complicated. For small φ_1, however, they can be expanded as power series in φ_1. Some details of the procedure are given in Appendix I, and the final expansions are:

$$E = e^{-\beta\pi}\left\{1 - \frac{1+\beta^2}{6}\left(\frac{\varphi_1}{2}\right)^2 + \frac{(1+\beta^2)(3+11\beta^2)}{360}\left(\frac{\varphi_1}{2}\right)^4 - \frac{(1+\beta^2)(9-6\beta^2+241\beta^4)}{45360}\left(\frac{\varphi_1}{2}\right)^6 \ldots\right\} \tag{3.13}$$

$$\varphi_m - \varphi_1 = \pi - \frac{\varphi_1}{2} + \frac{\beta}{3}\left(\frac{\varphi_1}{2}\right)^2 + \frac{\beta(1-\beta^2)}{45}\left(\frac{\varphi_1}{2}\right)^4 + \frac{\beta(3-10\beta^2+3\beta^4)}{1417{\cdot}5}\left(\frac{\varphi_1}{2}\right)^6 \ldots . \tag{3.14}$$

These series converge rapidly for a limited range of φ_1, and the degree of accuracy of (3.13) is shown in Fig. 8 for $\beta = 0$ and $\beta = 0{\cdot}5$. The curves marked '1st approx.' have been calculated taking only

two terms of the series, whilst 2nd and 3rd approximations correspond to three and four terms respectively. It is seen that, for φ_1 less than 2 (as usual in practice) the 1st approximation gives already an excellent accuracy.

In Ref. 1, the elevator was assumed to move according to the exponential formula:

$$\eta = -\eta_f(1-e^{-k\tau}), \tag{3.15}$$

so that the initial rate of elevator movement was $(-k\eta_f)$ and the 'mean rate' was assumed to be half that value:

$$\left(\frac{d\eta}{d\tau}\right)_{\text{mean}} = -\tfrac{1}{2}k\eta_f. \tag{3.16}$$

In our case of a trapezoidal elevator input {formula (3.6)}, the rate is constant:

$$\frac{d\eta}{d\tau} = -\frac{\eta_f}{\tau_1}. \tag{3.17}$$

If we want to make use of the assumptions of Ref. 1 as to the rates of elevator movement, we may simply equate (3.16) and (3.17), which gives:

$$\tau_1 = \frac{2}{k}, \text{ and hence } \varphi_1 = \frac{2J}{k}. \tag{3.18}$$

Czaykowski[1] assumes, on empirical grounds, that the *largest value of* k is:

$$k = 4J + R, \tag{3.19}$$

and thus we get the likely *smallest value of* φ_1:

$$\varphi_1 = \frac{2J}{4J+R}. \tag{3.20}$$

As R is usually much smaller than $4J$, this value differs very little from $0\cdot5$. For such rapid manoeuvres, the overshoot is almost exactly the same as for $\varphi_1 = 0$ (step input), cf. Fig. 6 and also, for comparison, Fig. 2b of Ref. 1. For some aircraft, the maximum rates of elevator movement may be expected to be considerably smaller, and then the alleviation in acceleration peaks will be significant. When using the formulae proposed in the present paper, we may simply assume the anticipated time t_1 (in seconds), and then determine:

$$\varphi_1 = Jt_1/\hat{t}, \tag{3.21}$$

where $\hat{t}$ is the unit of aerodynamic time.

4. *Incremental Incidence of the Tail, and Incremental Tail Loads.*

4.1. *Step Elevator Input.*

We have again $\eta = -\eta_f$ right from the start, and the operational formula (2.14) becomes:

$$\frac{\alpha_{\text{eff}}'}{\alpha_{\text{eff},f}'} = \frac{C + \dfrac{C\lambda}{J}D}{D^2 + 2RD + C}. \tag{4.1}$$

Its functional equivalent (cf. Ref. 3, form. 100) is:

$$\frac{\alpha_{\text{eff}}'}{\alpha_{\text{eff},f}'} = 1 - [\cos\varphi + \{\beta - \lambda(1+\beta^2)\}\sin\varphi]\,e^{-\beta\varphi} = \Phi'(\varphi) + \lambda\Phi''(\varphi), \tag{4.2}$$

and it is seen that this differs from (3.2) only by one modified coefficient. The difference is illustrated in Fig. 9, where the expression (4.2) has been plotted against φ, for $\beta = 0,\ 0{\cdot}2$ and for several values of λ {including $\lambda = 0$ which corresponds to form. (3.2)}. It is seen that the first peak value, which is the absolute maximum, occurs earlier and assumes higher values as λ increases. The effects may be quite small for aeroplanes with high wing loading flying at a great height, because μ is then large, and λ small. It may not necessarily be so in all cases, however, so that it is worth while to examine the matter in more detail. If we denote by $\varphi_m{}'$ the value at which the first peak occurs, and write:

$$\varphi_m{}' = \pi - \vartheta, \tag{4.3}$$

then it is shown in Appendix II that

$$\tan\vartheta = \frac{\lambda}{1-\beta\lambda}, \tag{4.4}$$

and the first peak value is given by:

$$\frac{\alpha'_{\text{eff},\max}}{\alpha'_{\text{eff},f}} = 1 + e^{-\beta\pi}E' = 1 + E_0E', \tag{4.5}$$

where E', the 'additional overshoot factor for tail incidence', is:

$$E' = e^{\beta\vartheta}\sqrt{\{1 - 2\beta\lambda + \lambda^2(1+\beta^2)\}} \tag{4.6}$$

The formulae (4.6) and (4.4) are illustrated in Figs. 10 and 11 for a range of values of β and λ. It is seen that $E' \geqslant 1$ (whereas $E \leqslant 1$) and may become quite large if both λ and β are large, but this will seldom be the case.

If λ is small, the formulae can be expanded in power series and, as shown in Appendix II, we have:

$$E' = 1 + \tfrac{1}{2}(1+\beta^2)\lambda^2 + \tfrac{2}{3}\beta(1+\beta^2)\lambda^3 + \tfrac{1}{8}(1+\beta^2)(7\beta^2-1)\lambda^4 + \tfrac{1}{15}(1+\beta^2)(17\beta^2-7)\lambda^5 \ldots . \tag{4.7}$$

4.2. *Trapezoidal Elevator Input.*

Applying the same procedure as in Section 3.2, the operational formula (2.14) becomes, for the 1*st part* of the manoeuvre:

$$\frac{\alpha'_{\text{eff}}}{\alpha'_{\text{eff},f}} = \frac{C(J+\lambda D)}{\varphi_1 D(D^2+2RD+C)}, \tag{4.8}$$

and the functional solution is:

$$\frac{\alpha'_{\text{eff}}}{\alpha'_{\text{eff},f}} = \frac{\Phi(\varphi) + \lambda\Phi'(\varphi)}{\varphi_1} \qquad (0<\varphi<\varphi_1), \tag{4.9}$$

where $\Phi(\varphi)$ and $\Phi'(\varphi)$ are functions defined by (3.8) and (3.2). During the 2*nd part* of the manoeuvre, we shall have:

$$\frac{\alpha'_{\text{eff}}}{\alpha'_{\text{eff},f}} = \frac{\Phi(\varphi) - \Phi(\varphi-\varphi_1) + \lambda\{\Phi'(\varphi) - \Phi'(\varphi-\varphi_1)\}}{\varphi_1} \qquad (\varphi>\varphi_1). \tag{4.10}$$

The explicit equivalents of (4.9) and (4.10) are given in full in Appendix III, and the formulae illustrated in Fig. 12 for $\beta = 0{\cdot}2$, $\lambda = 0{\cdot}5$ or 1, and several values of φ_1. Fig. 13 illustrates the case $\beta = 0$, $\lambda = 1$.

The first peak value of (4.10) is again the absolute maximum, and it may be obtained in a way similar to that used before (Section 3.2 and Appendix I). The calculation is somewhat involved, and some details are given in Appendix III, but the final result is surprisingly simple. The maximum becomes:

$$\frac{\alpha_{\text{eff}}{}'_{,\max}}{\alpha_{\text{eff}}{}'_{,f}} = 1 + EE', \tag{4.11}$$

so that the two previous overshoot factors must simply be multiplied; and the maximum occurs at

$$\varphi_m{}'' = \varphi_m - \vartheta \tag{4.12}$$

so that the maximum tail incidence leads the maximum normal acceleration by the same 'phase angle' ϑ, irrespective of the duration of the 1st part of the elevator manoeuvre.

The overshoot factor for the tail incidence (EE') depends on three parameters β, λ and φ_1. But, as it is a product of E and E' (each depending on two parameters only), two figures only, 5 (or 6) and 10, are sufficient to determine it in each particular case.

4.3. *Formula for Maximum Incremental Upload.*

Let us consider the more general case of the trapezoidal input, because the step input may be regarded simply as a special case, with $\varphi_1 = 0$.

The incremental load acting on the tail during the pull-out manoeuvre is:

$$P = \tfrac{1}{2}\rho V^2 S' C_L{}' = \tfrac{1}{2}\rho V^2 S'(a_1 \alpha_{\text{eff}}{}' + a_2 \eta), \tag{4.13}$$

and it reaches its maximum simultaneously with $\alpha_{\text{eff}}{}'$, some time after the elevator has been fully deflected to its final value ($-\eta_f$). We have* therefore:

$$P_{1\max} = \tfrac{1}{2}\rho V^2 S'(a_1 \alpha_{\text{eff}}{}'_{,\max} - a_2 \eta_f) \tag{4.14}$$

or, introducing (4.11) and (2.19):

$$P_{1\max} = \tfrac{1}{2}\rho V^2 S' a_2 \eta_f \left\{ \frac{a_1 \overline{V}}{a H_m} \left(1 - \frac{d\epsilon}{d\alpha} + \frac{a}{2\mu}\right)\left(1 + EE'\right) - 1 \right\}. \tag{4.15}$$

On the other hand, the weight of the aircraft in the initial equilibrium conditions (in level flight, or at a small inclination to the horizontal) may be considered as equal to the lift:

$$W = \tfrac{1}{2}\rho V^2 S C_L, \tag{4.16}$$

and the maximum incremental load factor, from (3.11) and (2.18) is:

$$n_{\max} = \frac{\overline{V}}{C_L H_m} a_2 \eta_f (1 + E). \tag{4.17}$$

Combining the last three equations, we obtain the final formula:

$$\frac{P_{1\max}}{W n_{\max}} = \frac{S' a_1}{S a}\left(1 - \frac{d\epsilon}{d\alpha} + \frac{a}{2\mu}\right)\frac{1 + EE'}{1 + E} - \frac{c H_m}{l(1+E)}, \tag{4.18}$$

which is most convenient, as the value of $n_{\max}$ is usually prescribed. The formula contains only

---

* This maximum load is denoted by $P_{1\max}$ (and often termed the 'first maximum incremental tail load') to make a distinction from the 'second maximum incremental tail load', $P_{2\max}$, which appears at a later stage of the 'standard manoeuvre'—*see* Section 7.1 (C).

fundamental design data and, in addition, only the two overshoot factors E and E', to be taken from Figs. 6 and 10. The second term still represents the effect of elevator deflection, the first one that of the aeroplane response.

In the case of a step input, the formula still applies, with E replaced by $E_0 = e^{-\beta\pi}$.

It may be noticed that, *if λ is small*, E' exceeds 1 only by a very small fraction, hence the fraction $(1+EE')/(1+E)$ in the first term of (4.18) is very nearly equal to 1, and may often be omitted. However, the fraction $1/(1+E)$ in the second term may be considerably smaller than 1, and should not be omitted generally, as it may contribute significantly to obtaining higher $P_{\max}$.

We may consider the *particularly simple special case, when the damping of the short-period oscillation is very high*, say $\beta > 1$. In such a case all overshoots may be ignored, and (4.18) becomes:

$$\frac{P_{1\max}}{Wn_{\max}} \approx \frac{S'a_1}{Sa}\left(1 - \frac{d\epsilon}{d\alpha} + \frac{a}{2\mu}\right) - \frac{cH_m}{l} = \frac{P_f}{Wn_f}, \tag{4.19}$$

but this may be simplified as follows. We have:

$$H_m = K_m - \frac{l}{c}\frac{m_q}{\mu}, \tag{4.20}$$

where the restoring margin K_m is:

$$K_m = h_0 - h + \bar{V}\frac{a_1}{a}\left(1 - \frac{d\epsilon}{d\alpha}\right), \tag{4.21}$$

and the damping derivative m_q, supposed to be provided by the tail only, may be written:

$$m_{q(\text{tail})} = -\tfrac{1}{2}\frac{S'}{S}a_1. \tag{4.22}$$

Substituting into (4.19), we find:

$$\frac{P_{1\max}}{Wn_{\max}} \approx \frac{c}{l}(h - h_0). \tag{4.23}$$

This formula may seem unbelievably simple. As a matter of fact, it follows directly from first principles, if we assume that the maximum tail load obtains when the equilibrium conditions in the steady circle have been established (thus neglecting overshoots during the transient period). The incremental wing load $Wn_{\max}$ is applied at the station ch_0, thus its positive moment about c.g. is $Wn_{\max}(ch - ch_0)$, while the negative moment of the incremental tail load is $P_{1\max}l$. Equating the two moments, we get (4.23) at once. The formula (4.23) is, of course, not recommended for use in detailed calculations.

By using (4.20 to 22), the full formula (4.18) can be manipulated into:

$$\frac{P_{1\max}}{Wn_{\max}} = \frac{c}{l}\left[(h - h_0)\frac{1+EE'}{1+E} + H_m\frac{EE'}{1+E}\right] + \frac{(m_q)_{wb}}{\mu}\frac{1+EE'}{1+E}, \tag{4.24}$$

where the last term contains the (previously neglected) damping derivative $(m_q)_{wb}$; this shows that the correct value normally exceeds that given by (4.23), the last term being usually very small. By elimination of H_m the formula (4.24) may also be written in the following form:

$$\frac{P_{1\max}}{Wn_{\max}} = \frac{1}{1+E}\left[\frac{c}{l}(h - h_0) + \frac{S'}{S}\frac{a_1}{a}\left(1 - \frac{d\epsilon}{d\alpha} + \frac{a}{2\mu}\right)EE'\right] + \frac{(m_q)_{wb}}{\mu(1+E)}, \tag{4.24a}$$

which may be often most convenient, as it contains only the very first design data, and overshoot factors.

4.4. *Formulae for Maximum Incremental Download.*

For the first part of the pull-out manoeuvre ($\varphi < \varphi_1$), we must introduce the following expression in the formula (4.13) for the incremental tail load:

$$\eta = -\eta_f \frac{\varphi}{\varphi_1} \tag{4.25}$$

and, according to (4.9) and (2.19):

$$\alpha_{\text{eff}}' = \frac{a_2 \overline{V}}{a H_m} \left(1 - \frac{d\epsilon}{d\alpha} + \frac{a}{2\mu}\right) \eta_f \frac{\Phi(\varphi) + \lambda \Phi'(\varphi)}{\varphi_1} \qquad (\varphi < \varphi_1). \tag{4.26}$$

We have therefore:

$$P = \tfrac{1}{2}\rho V^2 S' a_2 \frac{\eta_f}{\varphi_1} \left[\frac{1}{p}\{\Phi(\varphi) + \lambda \Phi'(\varphi)\} - \varphi\right] \qquad (\varphi < \varphi_1), \tag{4.27}$$

where:

$$p = \frac{a H_m}{a_1 \overline{V} \left(1 - \frac{d\epsilon}{d\alpha} + \frac{a}{2\mu}\right)}. \tag{4.28}$$

In the early stages of the manoeuvre, when φ is small and increasing, $\Phi'(\varphi)$ is small of 2nd order, as is easily seen from (3.2); hence $\Phi(\varphi)$ is small of 3rd order. In (4.27), therefore, the last term φ in brackets is initially the dominant one, and P is initially negative, its numerical value increasing up to a certain maximum.

It will be convenient again to relate the download to the maximum normal force $Wn_{\max}$, i.e. to combine (4.27) with (4.16) and (4.17). We may then write:

$$\frac{-P}{Wn_{\max}} = \frac{c H_m}{l(1+E)} \frac{F(\varphi)}{\varphi_1} \qquad (\varphi < \varphi_1), \tag{4.29}$$

where

$$F(\varphi) = \varphi - \frac{\Phi(\varphi) + \lambda \Phi'(\varphi)}{p}. \tag{4.30}$$

We have now to determine the *maximum download* which will be denoted by $(-P)_{\max}$. Let us observe first that, in the case of an *instantaneous elevator displacement* (*step input*) the greatest download occurs immediately at the start, and its value is given by the simple formula:

$$\frac{(-P)_{\max}}{Wn_{\max}} = \frac{c H_m}{l(1+E)} \qquad (\varphi_1 = 0). \tag{4.31}$$

This becomes obvious when considering the formula (4.18) for maximum upload. The second term in (4.18) is due to the elevator deflection alone, the first one to the aeroplane response and to the resulting increase of tail incidence. In the case of step input, only the second (negative) term applies initially, and this is expressed by (4.31).

The formula (4.31) gives an exaggerated value (which is still a very useful upper limit) whenever the elevator is deflected at a finite rate. To get a clear picture of the alleviation in various cases, the reader is referred to Fig. 20, which gives full response curves for the tail load, as calculated for the example of Section 6. For each φ_1, the curve consists of two parts, the initial one extending from $\varphi = 0$ to the 'terminal' point at $\varphi = \varphi_1$. All initial parts are expressed by the same equation (4.29) and thus only differ in scale which increases in inverse proportion to φ_1. The true turning points would therefore occur for the same value of φ, which will be denoted by φ^*.

For small φ_1 (less than φ^*), the initial parts of the curves never reach their turning points and, as the further parts deflect sharply upwards, the maxima are obtained simply by putting $\varphi = \varphi_1$:

$$\frac{(-P_{\max})}{Wn_{\max}} = \frac{cH_m}{l(1+E)} \frac{F(\varphi_1)}{\varphi_1} = \frac{cH_m}{l(1+E)} \left\{ 1 - \frac{\Phi(\varphi_1) + \lambda\Phi'(\varphi_1)}{p\varphi_1} \right\} \qquad (\varphi_1 < \varphi^*) . \quad (4.32)$$

This formula, involving only a very simple computation, is often all that is required when rapid elevator manoeuvres are to be reckoned with. When $\varphi_1 \to 0$, the ratio $F(\varphi_1)/\varphi_1 \to 1$, and we come back to (4.31). The general illustration is given in Fig. 14, where the upper graph shows a typical response curve $F(\varphi)$ and, for any φ_1 less than φ^* (such as φ_1' or φ_1''), the maxima of the ratio $F(\varphi)/\varphi_1$ of form. (4.29) are equal to the slopes of the respective secants (OQ′ or OQ″). The values are plotted in the lower graph (respective points P′, P″, etc., up to P* only). The initial ordinate OP_0 (slope of the tangent at O) is always equal to 1 and other ordinates represent the alleviation factor.

For larger φ_1 (greater than φ^*), the initial parts of the curves in Fig. 20 reach their turning points and extend beyond them, up to φ_1. The maxima of (4.29) become:

$$\frac{(-P)_{\max}}{Wn_{\max}} = \frac{cH_m}{l(1+E)} \frac{F(\varphi^*)}{\varphi_1} \qquad (\varphi_1 > \varphi^*), \quad (4.33)$$

where $F(\varphi^*)$ is independent of φ_1, so that these maxima vary simply in inverse proportion to φ_1, and the remainder of the lower curve in Fig. 14 is a hyperbola. Its ordinates (such as those of points P‴, P⁗) can be obtained from the upper curve as the slopes of lines (such as OQ‴, OQ⁗) joining the origin not with the points of the curve but with their projections (Q‴, Q⁗, etc.) on the horizontal tangent through Q*. The maxima decrease with rising φ_1, but always remain true downloads, while the formula (4.32) would not only underestimate the maxima but sometimes even give results with a wrong sign. Because of difference of procedure for small and large φ_1, the ordinates of the lower curve in Fig. 14 are denoted by $F(\varphi)_m/\varphi_1$ which means either $F(\varphi_1)/\varphi_1$ or $F(\varphi^*)/\varphi_1$, as the case may be.

The formula (4.33) requires a little more work than (4.32), as φ^* and $F(\varphi^*)$ must be found first. The usual procedure will be to compute the entire curve of $F(\varphi)$—some 6 or 8 points will normally suffice to have a fairly accurate plot, and then the procedure is straightforward.

It may be noticed that, *for any* φ_1, when φ exceeds φ_1, the equation (4.29) for the variation of tail load ceases to apply, and this will be given by:

$$\frac{P}{Wn_{\max}} = \frac{cH_m}{l(1+E)} \frac{F(\varphi-\varphi_1) - F(\varphi)}{\varphi_1} . \quad (4.34)$$

This formula should be used for computing the second parts of the tail loads curves beyond the 'terminal' points, as has been done in Fig. 20. The curves invariably deflect sharply upwards at these points.

Note. It is possible to avoid any curve tracing by using approximate formulae for φ^* and $F(\varphi^*)$. It is a difficult problem to derive such approximations, applicable to all sets of values of the three parameters (β, λ, p) involved, but convergent power series were worked out by Mr. D. N. Foster during his stay at the R.A.E. as vacation student. The series and a summary of their derivation are given in Appendix IV. The work was based on the assumption that $\sqrt{p}$ and $\lambda/\sqrt{p}$ were both small, but the series converge well for all values of the parameters which are likely to be encountered in practice. This is illustrated in Figs. 15 to 18, where the curves of $F(\varphi)$ and $F(\varphi)_m/\varphi_1$ are traced for a

number of values of β, $\lambda/\sqrt{p}$ and p. The exact turning points are shown, as well as approximate points (circled) calculated from (IV.6, 8). It is seen that only for quite large values of p and λ are the errors worth mentioning.

It is not expected that the series will be widely used, because of their rather complicated coefficients, so that the previous method of curve plotting will usually be preferred. The series, however, may be utilised for obtaining some very simple and useful *rough approximations*. Taking, for instance, only the first terms of each series, we obtain:

$$\varphi^* \approx \sqrt{\frac{2p}{1+\beta^2}},\quad F(\varphi^*) \approx \frac{2}{3}\sqrt{\frac{2p}{1+\beta^2}},\quad \text{and}\quad \frac{F(\varphi^*)}{\varphi^*} \approx \frac{2}{3}. \tag{4.35}$$

The ratio $F(\varphi^*)/\varphi^*$ is the alleviation factor for $\varphi_1 = \varphi^*$. The exact loci of this factor are shown in Figs. 15 to 18, and it is seen that this quantity varies little with p, and seldom differs much from 2/3, the errors being largest for the extreme case of very large β and very large $\lambda/\sqrt{p}$. The accuracy of the approximations for φ^* and $F(\varphi^*)$ is also tolerable, but not quite so good for large β.

5. *Normal Acceleration at Tail.*

This acceleration may be needed for determining inertial forces of the tail mass which alleviate the tail load. Another application may be found in interpreting flight tests, if a recording accelerometer is carried in the tail. It will be useful therefore to develop, as briefly as possible, formulae for this acceleration, the more so as it will be shown that similar methods and expansions apply successfully for determining the peaks, as used before for the tail incidence.

We consider again two cases, viz. step and trapezoidal elevator input.

(A) *Step elevator input.*

Assuming $\eta = -\eta_f$ right from the start, (2.15) becomes:

$$\frac{n_t}{n_f} = \frac{C - \frac{C}{\mu}D - \frac{2C}{\mu a}D^2}{D^2 + 2RD + C}, \tag{5.1}$$

and its functional equivalent (Ref. 3, form. 100):

$$\begin{aligned}\frac{n_t}{n_f} &= \Phi'(\varphi) - \frac{J}{\mu}\Phi''(\varphi) - \frac{2J^2}{\mu a}\Phi'''(\varphi)\\ &= 1 - \left[\left(1+\frac{2C}{\mu a}\right)\cos\varphi + \left\{\beta\left(1+\frac{2C}{\mu a}\right) - \frac{C(4R-a)}{\mu a J}\right\}\sin\varphi\right] e^{-\beta\varphi}.\end{aligned} \tag{5.2}$$

It may be noticed that, in this case, the initial value $n_{t,0}$ of the acceleration is not zero, because only $\Phi'(0) = \Phi''(0) = 0$, while $\Phi'''(0) = 1 + \beta^2 \neq 0$, and we have {using (2.16)}:

$$\frac{n_{t,0}}{n_f} = -\frac{2C}{\mu a} = -\frac{cH_m}{i_B l} \qquad \text{or, using (2.18):} \qquad n_{t,0} = -\frac{a_2 S'\eta_f}{i_B S C_L}, \tag{5.3}$$

as may also be checked from first principles. Form. (5.2) differs from (3.2) only by modified coefficients, but there are some new parameters involved, in particular μ and a. It might seem that (5.2) becomes very nearly identical with (3.2) for very large μ, but this is not so because C itself grows very nearly in proportion to μ {*see* (2.16)}, and J in proportion to $\sqrt{C}$ or $\sqrt{\mu}$. The quantity $C/\mu a$ is, however, a small fraction usually, so that the difference between (3.2) and (5.2) is not large, and some useful expansions in inverse powers of μa will be found below. The initial value of the

acceleration is negative and usually small in comparison with the final positive value. It is also easily checked that the acceleration starts increasing immediately and soon becomes positive, to oscillate afterwards about its final (asymptotic) value, with gradually decreasing amplitude. An example is given in Fig. 19, where the curve marked $\varphi_1 = 0$ applies in the present case, and may be usefully compared with the corresponding curve in the same figure representing the normal acceleration at c.g. for step input. It was assumed $\beta = 0$ or $\beta = 0{\cdot}2$, and $J/a = 2$, $J/\mu = 0{\cdot}08$, so that $2C/\mu a = 0{\cdot}3328$, a comparatively large value to get a clear picture. It is seen that the first peak value, which is the absolute maximum, assumes higher values than is the case for the c.g. normal acceleration. If we denote by φ_n' the value of φ at which the first peak occurs, and write:

$$\varphi_n' = \pi - \vartheta_n, \tag{5.4}$$

then it is shown in Appendix V that:

$$\tan\vartheta_n = \frac{J(4R-a)}{\mu a + 2C - R(4R-a)}, \tag{5.5}$$

and the first peak value is given by:

$$\frac{n_{t,\max}}{n_f} = 1 + e^{-\beta\pi}E_1, \tag{5.6}$$

where E_1, the 'additional overshoot factor for tail normal acceleration', is:

$$E_1 = e^{\beta\vartheta_n}\sqrt{\left\{\left(1+\frac{2C}{\mu a}\right)^2 - \left(\frac{2R}{\mu}+\frac{C}{\mu^2}\right)\left(\frac{4R}{a}-1\right)\right\}}. \tag{5.7}$$

It would be superfluous to try to illustrate formulae (5.5) and (5.7) for a comprehensive range of all parameters involved. It is clear, however, that ϑ_n is positive, i.e. the normal acceleration at the tail precedes that at c.g., whenever $4R > a$, which is always the case {cf. form. (2.5)} if $\nu + \chi > 0$, i.e. the total rotary damping of the aeroplane is positive. As to the overshoot factor E_1, it is shown in Appendix V to expand into the following series, in inverse powers of μa:

$$E_1 = 1 + \frac{2C}{\mu a} + \frac{C(4R-a)^2}{2\mu^2a^2} - \frac{C(4R-a)^2\{C - \frac{2}{3}R(4R-a)\}}{\mu^3a^3}\ldots., \tag{5.8}$$

which usually converges so rapidly that the first two terms are sufficient.

(B) *Trapezoidal elevator input.*

This case may be treated in a similar way as in Sections 3.2 and 4.2, and some details are given briefly in Appendix V. An illustration is given in Fig. 19, with the same values of constants as for the step input, and with several values of φ_1. It is seen that the acceleration is initially 0, assumes small negative values during a short period, and soon becomes positive to oscillate, with gradually decreasing amplitude, about the asymptotic value. The first peak value (absolute maximum) can be obtained as simply as in Section 4.2, viz.:

$$\frac{n_{t,\max}}{n_f} = 1 + EE_1, \tag{5.9}$$

so that the overshoot factors are simply multiplied; and the maximum occurs at

$$\varphi_n'' = \varphi_m - \vartheta_n, \tag{5.10}$$

so that the maximum normal acceleration at the tail leads that at c.g. by the same angle ϑ_n, irrespective of the duration of the first part of the elevator manoeuvre.

Combining (5.9) and (3.11) ,we get:

$$\frac{n_{t,\max}}{n_{\max}} = \frac{1 + EE_1}{1 + E}, \tag{5.11}$$

which shows that $n_{t,\max} > n_{\max}$, because E_1 is normally greater than 1 {cf. expansion (5.8)}. However, $n_{t,\max}$ usually exceeds $n_{\max}$ only slightly.

6. *Numerical Example.*

Let us consider the following numerical data, agreeing as exactly as possible with those used in Ref. 1, so as to have a direct comparison of our results with those obtained for the 'equivalent' exponential elevator input:

$$W = 15750 \text{ lb}, \quad V = 600 \text{ ft/sec}, \quad S = 350 \text{ sq. ft}, \quad c = 10{\cdot}5 \text{ ft},$$

$$S' = 54{\cdot}1 \text{ sq. ft}, \quad l = 20{\cdot}17 \text{ ft}, \quad i_B = 0{\cdot}1536,$$

height = 30,000 ft, hence $\sigma = 0{\cdot}374$, $\rho = 0{\cdot}000889$ slugs/cu. ft, $g\rho = 0{\cdot}0286$ lb/cu. ft.

We obtain:

$$\mu = \frac{W}{\rho g S l} = 78, \quad \hat{t} = \frac{W}{\rho g S V} = 2{\cdot}62 \text{ sec},$$

$$\tfrac{1}{2}\rho V^2 = 160 \text{ lb/sq. ft}, \quad C_L = \frac{W}{\tfrac{1}{2}\rho V^2 S} = 0{\cdot}2812;$$

$$\frac{S'}{S} = 0{\cdot}1545, \quad \frac{l}{c} = 1{\cdot}921, \quad \overline{V} = \frac{S'l}{Sc} = 0{\cdot}2968.$$

Let us assume further the following aerodynamic data:

$$a = 3{\cdot}291, \quad a_1 = 2{\cdot}8, \quad a_2 = 1{\cdot}75, \quad \frac{d\epsilon}{d\alpha} = 0{\cdot}55;$$

$$\omega = 43{\cdot}09 \text{ (corresponding to } K_m = \frac{2\omega i_B l}{\mu a c} = 0{\cdot}0990), \quad (m_q)_{\text{wing+fus.}} = -0{\cdot}18,$$

and calculate:

$$(m_q)_{\text{tail}} = -\frac{S'a_1}{2S} = -0{\cdot}2163, \quad m_{q(\text{total})} = -0{\cdot}3963, \quad \nu = -\frac{m_q}{i_B} = 2{\cdot}58,$$

$$m_{\dot{w}} = (m_q)_{\text{tail}} \frac{d\epsilon}{d\alpha} = -0{\cdot}1190, \quad \chi = -\frac{m_{\dot{w}}}{i_B} = 0{\cdot}7745, \quad \delta = 68{\cdot}65.$$

$$2R = \tfrac{1}{2}a + \nu + \chi = 5, \quad R = 2{\cdot}5; \quad C = \omega + \tfrac{1}{2}a\nu = 47{\cdot}335 \text{ (corresponding to}$$

$$H_m = \frac{2Ci_B l}{\mu a c} = 0{\cdot}1088); \quad J = \sqrt{(C - R^2)} = 6{\cdot}41; \quad \beta = R/J = 0{\cdot}39, \; e^{-\beta\pi} = 0{\cdot}2937.$$

Normal acceleration at c.g.

Assume $\eta_f = 17° = 0{\cdot}2966$ rad, then from (2.18) $n_f = 5{\cdot}036$. Also assume, as in Ref. 1, $k = 4J + R = 28{\cdot}14$, and hence, from (3.20) the corresponding $\varphi_1 = 0{\cdot}456$ rad, $\beta\varphi_1 = 0{\cdot}1777$, $e^{\beta\varphi_1} = 1{\cdot}1944$, $e^{-\beta\varphi_1} = 0{\cdot}8372$, $e^{-2\beta\varphi_1} = 0{\cdot}7009$. The overshoot can now be calculated according

to Section 3.2. The formula (3.12) yields: $\tan(\varphi_m-\varphi_1) = -0{\cdot}2248$, hence $\varphi_m-\varphi_1 = \pi - 0{\cdot}2212 = 2{\cdot}9204$, $\beta(\varphi_m-\varphi_1) = 1{\cdot}1390$, $e^{-\beta(\varphi_m-\varphi_1)} = 0{\cdot}3201$, and finally from (3.11), $E = 0{\cdot}2907$ {the series in (3.13) gives the same value} and $n_{\max} = 6{\cdot}500$, as required in Ref. 1. Obviously, any arbitrary value of $n_{\max}$ may be obtained by simply scaling η_f up or down in proportion.

If the elevator were displaced instantaneously ($\varphi_1 = 0$), the overshoot factor would be $E_0 = e^{-\beta\pi} = 0{\cdot}2937$, and $n_{\max} = 6{\cdot}515$, only insignificantly higher value than 6·5. We may, however, take a number of greater values of φ_1, obtaining the following results:

TABLE 1

φ_1	$\tan(\varphi_m-\varphi_1)$	$\varphi_m-\varphi_1$	$e^{-\beta(\varphi_m-\varphi_1)}$	E	$n_{\max}$	τ_1	t_1(sec)
0	0	3·1416	0·2937	0·2937	6·515	0	0
0·456	−0·2248	2·9204	0·3201	0·2907	6·500	0·0711	0·186
0·800	−0·3983	2·7626	0·3405	0·2848	6·470	0·1248	0·327
1·200	−0·6162	2·5894	0·3642	0·2739	6·415	0·1872	0·490
1·600	−0·8659	2·4280	0·3879	0·2593	6·342	0·2496	0·654
2·000	−1·1668	2·2794	0·4111	0·2416	6·253	0·3120	0·817
2·400	−1·5447	2·1453	0·4331	0·2213	6·150	0·3744	0·981
∞	—	—	—	0	5·036	∞	∞

The computation has been made using the exact formula (3.11), but the series in (3.13) leads to identical results, with only very slight inaccuracies for large φ_1. It is seen that, even in the case of a sluggish input of ~1 sec. duration, the maximum acceleration only decreases by about 6%.

Incremental tail incidence and tail upload.

Here we need the additional parameter λ {form. (2.8)}.

$\lambda = 0{\cdot}2704$, and hence, from (4.4) and (4.6): $\tan\vartheta = 0{\cdot}3023$, $e^{\beta\vartheta} = 1{\cdot}1213$,

$\varphi_m' = \pi - 0{\cdot}2936 = 2{\cdot}8480$ rad, $E' = 1{\cdot}1213 \times 0{\cdot}9345 = 1{\cdot}0479$.

This enables us to calculate maximum tail incidence and maximum tail upload for any φ_1, using (4.11) and (4.18). We first determine the final values:

from (2.19): $\alpha_{\text{eff},f}' = 0{\cdot}2027$ rad $= 11{\cdot}62°$,

from (4.19): $\dfrac{P_f}{n_f} = 975 - 892 = 83$ lb,

and then (4.11) and (4.18) become, respectively:

$$\alpha_{\text{eff},\max}' = 0{\cdot}2027\,(1+EE'), \tag{6.1}$$

$$\frac{P_{1\max}}{n_{\max}} = 975\,\frac{1+EE'}{1+E} - \frac{892}{1+E}, \tag{6.2}$$

which, in conjunction with Table 1, leads to the following results:

TABLE 2

φ_1	$1 + EE'$	$\alpha_{\text{eff}}', \max$ radians	$\frac{P_{1\max}}{n_{\max}}$ lb	$P_{1\max}$ lb for $\eta = 17°$	$P_{1\max}$ lb for $n_{\max} = \text{const.} = 6{\cdot}5$
0	1·3078	0·2653	296	1928	1924
0·456	1·3046	0·2646	294	1911	1911
0·800	1·2984	0·2634	291	1883	1892
1·200	1·2870	0·2609	285	1828	1853
1·600	1·2717	0·2580	276	1750	1794
2·000	1·2532	0·2541	266	1663	1729
2·400	1·2319	0·2498	253	1556	1645
∞	1	0·2027	83	418	540

It is seen, as could be expected, that the maximum incremental incidence does not vary much with φ_1, but the variation in the maximum tail upload is considerable, and the effects of overshoots very important. It must be mentioned that the values of the ratio $P_{1\max}/n_{\max}$ in the 4th column of Table 2 have been calculated from (4.18) or (6.2) taking the appropriate E in each case, so that $n_{\max}$ is somewhat different for each value of φ_1, as in Table 1. The values of $P_{1\max}$ thus correspond strictly to the assumed elevator deflection (17°). If the elevator angle were adjusted in each case so as to obtain constant $n_{\max} = 6{\cdot}5$ for any φ_1, then the load $P_{1\max}$ would assume somewhat different values, tabulated in the last column. The differences are small in this example, except for $\varphi_1 = \infty$, i.e. for the asymptotic value, for which all overshoots are omitted. The present example is illustrated by Fig. 20, where the time histories of tail load per constant $n_{\max}$ (6·5) have been plotted. The positive peak values thus correspond to the last column of Table 2. The figure corresponds to Fig. 2h of Ref. 1, and a fair agreement of the peak values is clearly seen.

Incremental download on tail.

Here the additional parameter p is needed, which is obtained from (4.28):

$$p = 0{\cdot}915$$

In the case of *step input*, we find from (4.31), taking $n_{\max} = 6{\cdot}5$, $E = 0{\cdot}2907$:

$$\frac{(-P)_{\max}}{n_{\max}} = 690 \text{ lb}, \quad (-P)_{\max} = 4492 \text{ lb},$$

this corresponding to the initial ordinate of the curve marked $\varphi_1 = 0$ in Fig. 20. For this and other values of φ_1, full response curves have been produced using equations (4.29) and (4.30) which take the form:

$$-\frac{P}{n_{\max}} = 690\,\frac{F(\varphi)}{\varphi_1}, \qquad F(\varphi) = -0{\cdot}093\varphi + 0{\cdot}445 + (0{\cdot}919\sin\varphi - 0{\cdot}445\cos\varphi)e^{-0{\cdot}39\varphi}.$$

It is seen that for several smaller values of φ_1, the maximum downloads coincide with the ends of elevator movement; for higher φ_1 (2 and 2·4) the maximum download occurs before the elevator has been fully deflected, and it is a true turning value. The value $\varphi_1 = 1{\cdot}6$ seems to be the critical one coinciding with the true turning point, although the exact maximum occurs for $\varphi \approx 1{\cdot}497$.

The maxima are tabulated as follows:

TABLE 3

φ_1	$(-P)_{max}/n_{max}$ lb	$(-P)_{max}$, lb for n_{max} = const. = 6·5
0	690	4485
0·456	616	4004
0·800	540	3510
1·200	442	2873
1·600	343	2230
2·000	274	1781
2·400	229	1489

It is seen from Table 3 and Fig. 20 that the effect of φ_1 on the maximum download is very large indeed so that, when the duration of the input varies from 0 to about 1 second, the maximum download falls to one third of its initial value. In the given case, maximum incremental downloads considerably exceed maximum incremental uploads in rapid manoeuvres, but the position becomes reversed for more sluggish manoeuvres. Comparing Fig. 20 with Fig. 2h of Ref. 1, we notice that the trends are in good agreement, but our peak values are comparatively higher (e.g. we obtain 616 for $\varphi_1 = 0{\cdot}456$, while in Ref. 1 we find only about 500 for the corresponding value $[d\eta/dt] = 91{\cdot}4$). The differences in peak values are clearly due to the different shapes of the elevator time histories assumed for the two methods. The download peak occurs early in the manoeuvre, when both elevator deflection and response differ appreciably. In the case of instantaneous elevator input both methods obviously give the same value (4.31) due to the full elevator deflection alone. In the general case, the total download equals the difference between the force due to elevator deflection and that due to aeroplane response. The exponential elevator deflection, and its mean rate as assumed in Ref. 1, are given by (3.15, 16), while in the case of trapezoidal input, with the same rate during the initial part, we have:

$$\left.\begin{aligned} \eta_{tr} &= -\tfrac{1}{2}k\eta_f\tau \quad (\tau \leqslant \tau_1 = 2/k) \\ \eta_{tr} &= -\eta_f \qquad (\tau \geqslant \tau_1) \end{aligned}\right\}. \tag{6.3}$$

It is easily seen that η_{exp} has initially greater numerical values than η_{tr}, the ratio falling from 2 to 1 as τ increases up to $0{\cdot}7968\tau_1$ (when the common value $= -0{\cdot}7968\eta_f$); later the position is reversed (e.g., for $\tau = \tau_1$, we have $\eta_{tr} = -\eta_f$, $\eta_{exp} = -0{\cdot}8647\eta_f$) but, as τ goes on increasing, the ratio tends quickly to 1. For sufficiently rapid manoeuvres (k sufficiently large, τ_1 and φ_1 correspondingly small) the peak download resulting from trapezoidal input occurs at $\varphi = \varphi_1 (< \varphi^*)$, where $|\eta_{tr}| > |\eta_{exp}|$, while the response effects are still small, and thus we may expect the peak download to be greater. The differences are negligible for *very* small φ_1, but increase for somewhat larger φ_1 (e.g. in our example, our method gives some 20% greater peak value for $\varphi_1 = 0{\cdot}456$). As φ_1 is increased still further, the differences soon decrease and even change sign, while being very small and tending to 0. There is no point in pursuing the comparison in great detail because the assumption of equal mean rates is artificial anyhow. In cases when the trapezoidal input is an obviously realistic approximation, e.g. automatic-pilot 'runaway'[15], our formulae for peak download are, of course, directly applicable, the elevator rate corresponding to the maximum servomotor rate being the appropriate one.

It may be noticed that the method of this paper is particularly convenient for estimating the effects of varying rapidity of manoeuvre on the magnitude of tail loads during the initial stages, i.e. for $\varphi \leqslant \varphi_1$ (thus, in particular, of maximum downloads), without making new response calculations for any new value of the parameter φ_1. Thus the relevant portions of response curves, such as those in Fig. 20, must merely be scaled up or down, in inverse proportion to φ_1—*see* form. (4.29) where $F(\varphi)$ does not depend on φ_1.

Normal acceleration at tail.

In the case of *step elevator input*, we have, from (5.3) to (5.7), initial values: $n_{t,0}/n_f = -0{\cdot}3687$, $n_{t,0} = -1{\cdot}857$, and, for the first positive maximum: $\tan\vartheta_n = 0{\cdot}1285$, $\vartheta_n = 0{\cdot}1276$, $E_1 = 1{\cdot}0511 \times 1{\cdot}3142 = 1{\cdot}3814$, $n_{t,\max}/n_f = 1{\cdot}4057$, $n_{t,\max} = 7{\cdot}079$, so that this maximum exceeds that of the normal acceleration at c.g. (6·515), but only by some 9%. For *trapezoidal elevator input*, we use (5.9), and the results are tabulated below:

TABLE 4

φ_1	$n_{t,\max}/n_f = 1 + EE_1$	$n_{t,\max}$	$n_{t,\max}/n_{\max}$
0	1·4057	7·079	1·0866
0·456	1·4016	7·058	1·0859
0·800	1·3934	7·017	1·0845
1·200	1·3784	6·942	1·0820
1·600	1·3582	6·840	1·0785
2·000	1·3337	6·717	1·0742
2·400	1·3057	6·576	1·0691
∞	1	5·036	1

7. *Discussion.*

It has been shown that, on the assumption of step or trapezoidal elevator input, the normal accelerations at the c.g. and the tail, the incremental up- and downloads on the tail and, in particular, the important peak values of all these quantities can be easily determined. All results have been presented as simple formulae in terms of basic design data, so that rough preliminary computations can be performed even in the earliest design stage, and repeated more accurately in any later stage, as soon as more precise data become available. As the method neglects the variation of forward speed, it is applicable for all heights and flight speeds (sub-, trans- and supersonic), the effects of compressibility at high Mach numbers being reflected only through appropriate numerical values of the few aerodynamic derivatives involved. The important feature is the part played by the maximum value $n_{\max}$ of the normal acceleration at the c.g., which is normally stipulated in the aircraft specification; all other quantities, including in particular tail loads, have been related to it. It is assumed that the pilot will never exceed $n_{\max}$, and it would be extravagant to assume tail loads in excess of those which accompany this peak acceleration and corresponding main wing load. However, the matter requires some additional deliberation.

Although the formulae for maximum incremental tail loads are simple enough, two difficulties arise. *Firstly*, several parameters involved vary with flight conditions (weight, c.g. position, height, and speed or Mach number) for an existing aeroplane, or for a planned one with assumed main design data. It appears that the formulae should be applied in a great many different cases (several heights combined with several speeds and several c.g. positions), so as to enable us to pick out the highest values of the maxima. *Secondly*, an even more complicated problem arises in the early design stage, when the basic data are being discussed and decided. It may then be required that these data should lead to as small tail loads as possible or, if this is impracticable in view of some other overriding requirements, the effect of various choices on tail loads should at least be understood and taken into account. To clarify both matters, the main formulae will now be examined in detail.

7.1. *An aeroplane with Fixed Basic Design Data.*

(A) *Maximum incremental tail upload.*

The formula (4.18), which shows separate effects of tail deflection and response, is not very convenient for discussion, because some factors of the first term affect the value of manoeuvre margin H_m appearing in the second term. We shall therefore use form. (4.24a) which gives a clear picture of the effects of basic parameters.

The ratios S'/S and c/l are constants independent of flight conditions, but the remaining parameters do vary with them, and it is essential to consider their worst combinations leading to the highest $P_{1\max}$. The two terms derived from rotary damping m_q, namely the last term and that containing $a/2\mu$ are normally much smaller than the rest, and their effect is of little importance. Roughly, the upload may increase when:

(i) W rises to its greatest value,

(ii) h rises to its greatest value (i.e. *c.g. in its rearmost position*),

(iii) $\frac{a_1}{a}\left(1-\frac{d\epsilon}{d\alpha}\right)$ rises to its greatest value,

(iv) h_0 falls to its smallest value,

(v) E and E' rise to their greatest values.

It appears therefore that maxima in the case of greatest a.u. weight and rearmost c.g. position must be mainly considered*. Further, the values of $(a_1/a)(1-d\epsilon/d\alpha)$ and h_0, which depend primarily on Mach number, should be known and examined throughout its full range. No general discussion is possible here, but it should be stressed that these quantities may vary considerably as Mach number increases to transonic and supersonic values, and this variation should be carefully taken into account.

---

* This conclusion is strictly valid only if the weight and/or c.g. position are changed independently of each other (e.g., when loads are added without affecting c.g. position, or if some loads are shifted longitudinally). It often happens, however, that the two quantities vary simultaneously, for instance when fuel is consumed or added, and then the relationship between W and h must be known, and the formula (4.24a) examined taking this relationship into account (usually by drawing a graph), so as to find the greatest tail load, which may then not correspond to greatest W or greatest h. Strictly, the overshoot factors E, E' may also vary somewhat with W and h, and this may also be accounted for in this examination.

The effect of overshoot factors E, E' is of particular interest. Of those, E (always between 0 and 1) depends on β and φ_1, and E' (always greater than 1) on β and λ. If we re-write (4.24a), neglecting two small damping terms, in the form:

$$\frac{P_{1\max}}{Wn_{\max}} \approx \frac{\frac{c}{l}(h-h_0) + \frac{S'}{S}\frac{a_1}{a}\left(1-\frac{d\epsilon}{d\alpha}\right)EE'}{1+E}, \tag{7.1}$$

it is seen that this *does increase with* E, other quantities being assumed constant, provided

$$\frac{S'}{S}\frac{a_1}{a}\left(1-\frac{d\epsilon}{d\alpha}\right)E' > \frac{c}{l}(h-h_0)$$

or

$$h_0 - h + \frac{a_1}{a}\bar{V}\left(1-\frac{d\epsilon}{d\alpha}\right)E' > 0, \tag{7.2}$$

and (7.2) is always true because the left-hand part becomes equal (to the same degree of approximation) to manoeuvre margin H_m when $E' = 1$, and the true E' always exceeds 1. Also, (7.1) obviously *increases with* E'. In many cases, especially if the wing loading is high, and particularly at great heights, μ becomes large and λ small, hence E' exceeds 1 only slightly (cf. Fig. 10) and may often be replaced by 1. The effect of E, however, is always important. As this rises when φ_1 (or t_1) decreases (cf. Fig. 6), the *smallest foreseeable* φ_1 *should be considered.* The height affects the index $\beta = R/J$ because, with increasing height, R remains unaltered while J increases roughly in proportion to $\sqrt{\mu}$ or in inverse proportion to $\sqrt{\rho}$. Therefore, with *increasing height*, β becomes smaller and E larger, so that we might expect more and more dangerous uploads. This, however, seems odd: the higher we fly, the less violent manoeuvres are to be expected until, at the ceiling, a pull-out manoeuvre should never be performed. The explanation of the matter is simple but leads to important conclusions.

To reach the required $n_{\max}$, the wing must reach an appropriately *increased incidence*, such as to make its lift coefficient equal to

$$C_L + (\Delta C_L)_{\max} = C_L(1+n_{\max}). \tag{7.3}$$

This value, however, may often be unobtainable, and especially so at great heights, where the original C_L in undisturbed flight is already large, so that (7.3) may exceed the stalling value. In practice, the pilot will always avoid stalling and keep his increased C_L not higher than some limiting value $\bar{C}_L$ (usually less than $C_{L,\,\text{stall}}$, unless momentary increase above that value in rapid manoeuvres must be reckoned with), and then $n_{\max}$ should satisfy the inequality:

$$n_{\max} \not> \frac{\bar{C}_L - C_L}{C_L} \tag{7.4}$$

This limitation of $n_{\max}$ (which, of course, means a proportional limitation of η_f) may be very significant at low speeds and/or great heights, and must never be forgotten.

Let us apply this to our example of Section 6. The specified $n_{\max}$ was $6\cdot5$ and the initial undisturbed $C_L = 0\cdot2812$ (a rather high value for the speed of 600 ft/sec, due to the considerable height). The value of C_L required to reach the specified $n_{\max}$ would be, according to (7.3):

$$0\cdot2812 \times 7\cdot5 \approx 2\cdot1$$

which is obviously unobtainable. We must, therefore, assume a reasonable limiting value, say $\bar{C}_L = 1{\cdot}1$, and then, from (7.4), reduce our incremental load factor to

$$n_{\max} = \frac{1{\cdot}1 - 0{\cdot}2812}{0{\cdot}2812} = 2{\cdot}91\text{, instead of } 6{\cdot}5\text{!}$$

The values of $P_{1\max}$ listed in the last column of Table 2 in Section 6, must therefore be considered as grossly exaggerated. The remainder of the computation is, however, correct, so that the column of the ratio $P_{1\max}/n_{\max}$ need not be altered. The realistic values of $P_{1\max}$ will be as given in Table 5 at the end of the present Section 7.1, and they become very much lower than those previously estimated. The limit 2·91 for $n_{\max}$, however, only applies to the given height and speed, but not to lower heights and/or higher speeds. E.g. for the same speed at sea level, C_L would be reduced to 0·1718, and (7.4) would give $n_{\max} \approx 5{\cdot}4$, still less than 6·5. Even with somewhat smaller values of E and E', the final uploads will be much greater than in Table 5, but still less than those in Table 2. If speeds greater than 600 ft/sec could be reached, the value $n_{\max} = 6{\cdot}5$ might become realistic.

It may be stated generally that the value of $n_{\max}$ should never be assumed arbitrarily prior to ascertaining *what is the smallest C_L that can be reached in flight.* Now, C_L may decrease in descent, but only very little in ordinary shallow dives. If, however, the aeroplane is expected to perform steep or even vertical dives, C_L may decrease considerably even down to zero, and *in such cases (thus generally for fighters) the full specified $n_{\max}$ should be taken.*†

It must be stressed that the above remarks do not impair in the slightest measure the validity of the basic theory and formulae of this report (or of Ref. 1), and the only new conclusion is that concerning the limitation of $n_{\max}$ according to circumstances. And it may happen in practice that the greatest tail load will occur at low or medium rather than at great altitudes.

(B) *Maximum incremental tail download.*

We have the alternative formulae (4.32) and (4.33) for rapid or slow manoeuvres, respectively. These formulae do not include so many parameters, and are easily interpreted. The download may increase‡ when:

(i) W rises to its greatest value,

(ii) H_m increases to its greatest value, which happens for smallest h (*c.g. in its foremost position*) and when the quantity

$$h_0 + V\frac{a_1}{a}\left(1 - \frac{d\epsilon}{d\alpha}\right)$$

is the greatest that can possibly occur,

(iii) E decreases; this is due to the factor $(1+E)$ in the denominator, and the effect is opposite to that in the case of upload. It may be noticed, however, that there is some effect of varying E and λ on the ratio $F(\varphi_1)/\varphi_1$ or $F(\varphi^*)/\varphi_1$, which may be studied in Figs. 15 to 18.

In addition, the previous remarks about the limitation of $n_{\max}$ apply here just as for the uploads, and thus the greatest downloads will normally occur at lower rather than greater heights.

---

† For steep dives, the system of equations (2.1, 2) should, strictly speaking, be replaced by a somewhat more complicated one, but the formulae of this paper may still be used, with only trifling errors, provided C_L is replaced by $\sqrt{(C_L{}^2 + C_D{}^2)}$ or, in the limiting case of vertical dives, by C_D.

‡ The footnote to Section 7.1 (A) applies here.

As to our example of Section 6, we should assume again, for consistency, $n_{\max} = 2{\cdot}91$, and then the values of $(-P)_{\max}$ given in the last column of Table 3 in Section 6 will be much reduced, as shown in Table 5 at the end of the present Section 7.1.

(C) *Second maximum incremental tail upload.*

Up to now, we have only considered the first stage of the pull-out manoeuvre, which would leave the elevator with a full deflection η_f, and the aircraft in the steady circling condition, with n and P constant at their asymptotic values. However, the manoeuvre is normally completed by applying the elevator in the opposite direction, so as to bring the aircraft back to steady level flight. Ref. 1 stipulates the following assumptions as to this second stage of the manoeuvre. Prior to the reversed elevator movement, the aircraft is supposed to be in a steady circling attitude with the normal acceleration $n_{\max}g$ (thus somewhat greater than the asymptotic value), and with the corresponding tail upload. The reversed elevator movement is supposed to be the same as the initial one, i.e. with the same mean rate and maximum angle, but with reversed sign. The normal acceleration is then reduced to zero at its minimum, and the tail load acquires further increments exactly as in the first stage but with reversed sign, and these are added to the steady circling upload. There occurs therefore a second maximum incremental upload which is the sum of the steady circling one and of one equal to the maximum download of the first stage.

The expression for the *steady incremental upload in circling conditions* is obtained simply by neglecting overshoot (i.e. putting $E = 0$) in any of the formulae (4.18, 24, 24a), thus:

$$\frac{P_c}{Wn_{\max}} = \frac{c}{l}(h-h_0) + \frac{(m_q)_{wb}}{\mu} \tag{7.5}$$

and, adding to this either of the expressions (4.32, 33), we obtain the *2nd maximum incremental upload*:

$$\frac{P_{2\max}}{Wn_{\max}} = \frac{c}{l}(h-h_0) + \frac{(m_q)_{wb}}{\mu} + \frac{cH_m}{l(1+E)}\frac{F(\varphi)_m}{\varphi_1}, \tag{7.6}$$

where $F(\varphi)_m$ denotes either $F(\varphi_1)$ or $F(\varphi^*)$, depending on whether $\varphi_1 \gtrless \varphi^*$. It is easily checked that (7.5) is always somewhat smaller than the 1st maximum; the 2nd maximum (7.6) is, however, normally greater than the 1st one.

(D) *Static initial load and total load.*

It must never be forgotten that, up to now, we have only considered *incremental* tail loads, but the static load which is seldom 0 in undisturbed flight must always be taken into account. The *total loads* in the two cases will be:

$$\text{Maximum total upload } P_{\text{tot},1\max} = P_{1\max} + P_{\text{st}}, \tag{7.7}$$

$$\text{Maximum total download } (-P_{\text{tot}})_{\max} = (-P)_{\max} - P_{\text{st}}, \tag{7.8}$$

where P_{st} is the static tail load (positive when up), and may be simply obtained from trim conditions as

$$P_{\text{st}} = W\frac{c}{l}\left(h - h_0 + \frac{C_{m0}}{C_L}\right). \tag{7.9}$$

C_{m0} was often negative and appreciable in the old days, but it is usually near to 0 for more recent aeroplanes. Thus, P_{st} will normally be positive when $h > h_0$, i.e. c.g. behind the aerodynamic centre (and *vice versa*, which is not a rare case nowadays). It is positive in our example of Section 6, where

$$h - h_0 = \bar{V}\frac{a_1}{a}\left(1 - \frac{d\epsilon}{d\alpha}\right) - K_m = 0{\cdot}0146, \text{ hence (assuming } C_{m0} = 0)\ P_{st} = 120 \text{ lb.}$$

P_{st} obviously increases with W and h, thus becoming larger when the c.g. moves back; it may also vary with h_0 and C_{m0} and thus with Mach number.

Introducing the expressions for maximum incremental loads {(4.24) for the first maximum upload, (7.6) for the second maximum upload, (4.32) or (4.33) for the maximum download}, and for the static load (7.9), into (7.7) or (7.8), we obtain:

1st maximum total upload:

$$\frac{P_{\text{tot, 1 max}}}{Wn_{\max}} = \frac{c}{l}\left[(h-h_0)\left(\frac{1}{n_{\max}} + \frac{1+EE'}{1+E}\right) + \frac{C_{m0}}{C_L n_{\max}} + H_m\frac{EE'}{1+E}\right] + \frac{(m_q)_{wb}}{\mu}\frac{1+EE'}{1+E}; \quad (7.10)$$

2nd maximum total upload:

$$\frac{P_{\text{tot, 2 max}}}{Wn_{\max}} = \frac{c}{l}\left[(h-h_0)\left(\frac{1}{n_{\max}} + 1\right) + \frac{C_{m0}}{C_L n_{\max}} + \frac{H_m}{1+E}\frac{F(\varphi)_m}{\varphi_1}\right] + \frac{(m_q)_{wb}}{\mu}; \quad (7.11)$$

Maximum total download:

$$\frac{(-P_{\text{tot}})_{\max}}{Wn_{\max}} = \frac{c}{l}\left[\frac{H_m}{1+E}\frac{F(\varphi)_m}{\varphi_1} - \frac{1}{n_{\max}}\left(h - h_0 + \frac{C_{m0}}{C_L}\right)\right]. \quad (7.12)$$

These formulae seem to be most suitable for calculating tail loads. They should be tabulated for several heights through the range of speed, introducing in each case aerodynamic data corresponding to relevant Mach numbers, smallest foreseeable φ_1, and such compatible values of W, h, μ, E, E' as lead to greatest values of the loads; $n_{\max}$ should be either the specified value, or the limiting value (7.4) if this is smaller. Finally, graphs of the maximum total tail loads against V for various heights will reveal the true greatest maxima, to be used in stress calculations. Many simplifications of this rather complicated-looking procedure will undoubtedly be practicable in actual work, but this may be best left to practice and experience.

For our example, the values of incremental and total tail loads (including the 2nd maximum total upload), corresponding to the height 30,000 ft, speed 600 ft/sec, $n_{\max} = 2{\cdot}91$, $h - h_0 = 0{\cdot}0146$, and $C_{m0} = 0$, are listed below:

TABLE 5

φ_1	$P_{1\ \max}$ lb	$(-P)_{\max}$ lb	$P_{\text{tot, 1 max}}$ lb	$(-P_{\text{tot}})_{\max}$ lb	$P_{\text{tot, 2 max}}$ lb
0	861	2008	1081	1888	2371
0·456	856	1793	976	1673	2156
0·8	847	1571	967	1451	1934
1·2	829	1286	949	1065	1548
1·6	803	998	923	877	1360
2	774	797	894	677	1160
2·4	736	666	856	546	1029
∞	242	—	362	—	—

The 2nd maximum total upload is seen to be the greatest in all cases.

7.2. *An Aeroplane in the Early Stages of Design.*

Fundamentally, the discussion of 7.1 applies here, with various parameters estimated as well as possible, but the choice of the ratios S'/S and l/c is still open. Now, the tail volume ratio $\bar{V}$ must be chosen such that, with the anticipated range of h, the restoring margin (4.21) and manoeuvre margin (4.20) assume reasonable positive values in a desired range. The required $\bar{V}$ can normally be achieved by choosing either greater S'/S and smaller l/c, or *vice versa*. Greater values of l/c lead to improved damping which is desirable in itself, and also to smaller tail loads, because all important terms in (7.10) to (7.12) contain the factor c/l. We must not forget, however, that the fuselage bending moments will be obtained by multiplying (7.8) and (7.9) by l and, with a fixed $\bar{V}$, they will not depend on the choice of l/c and S'/S (except through overshoot factors). There will usually be some other reasons affecting the choice, but its effect on loads should not be overlooked.

7.3. *Ultimate Tail Loads after a Long Time, including Variation of Speed.*

The variation of forward speed has been consistently neglected up to now, on the assumption that the pull-out manoeuvre lasts only a short time (after which the stick is eased), and the conditions in Gates' steady circle can be considered as final. If, however, the manoeuvre lasts sufficiently long then, introducing full linear equations of motion (thus quartic stability equation, and phugoid mode), we obtain different asymptotic conditions, with speed decreased, incidence and attitude angle increased, and flight angle normally increased. The tail load then also tends to a certain asymptotic steady value, and it may be interesting to know whether this can exceed the maxima as determined before. The investigation, summarized in Appendix VI, shows that this depends on the static margin which, in a sense, then replaces the manoeuvre margin. The results may be very different in particular cases but, in manoeuvres involving large normal accelerations in early stages, the aeroplane will usually stall before reaching the final asymptotic conditions, or the final equilibrium will occur at speed so much reduced as to make the linear theory inapplicable. It is highly improbable that the loads at decreased speed exceed those in the high-speed manoeuvres.

7.4. *Remarks on Overshoot Factors.*

The overshoot factors have been determined for three incremental response quantities: normal acceleration at c.g., tail incidence, and normal acceleration at tail. In the first case, the operational formula was a fraction of 2nd order in D, with merely a constant in the numerator, and the maximum overshoot was E_0 (at $\varphi = \pi$) in the case of step input, and E (at $\varphi = \varphi_{n1}$) for trapezoidal input. For tail incidence the operational formula (2.9) was another fraction of 2nd order with the same denominator and a numerator linear in D, and the maximum overshoot was E_0E' (at $\varphi = \pi - \vartheta$) for step, and EE' (at $\varphi = \varphi_{n1} - \vartheta$) for trapezoidal input. Finally, for normal acceleration at tail, the operational formula (2.10) was yet another 2nd order fraction, with the same denominator and with a fully quadratic numerator; the overshoot was E_0E_1 (at $\varphi = \pi - \vartheta_n$) for step, and EE_1 (at $\varphi = \varphi_m - \vartheta_n$) for trapezoidal input. In both 2nd and 3rd cases, the overshoot factor for trapezoidal input was equal to E multiplied by the overshoot factor for step input, and the time angle led φ_m by the same amount (ϑ or ϑ_n, respectively) no matter what the duration (φ_1) of the elevator motion. Thus, both overshoot factor and time angle have to be determined only for step input, and then those for trapezoidal input can be obtained by simple multiplication and addition. The question arises how general this is, i.e. whether it applies to any other response quantities. The answer is that it does

for all quantities where operational equivalents are similar 2nd order fractions with an *arbitrary numerator* (order, of course, not exceeding 2), i.e. for all quantities which are linear combinations of $\hat{w}$, $\hat{q}$,and their derivatives (also η_f if necessary), but excluding their integrals. The proof consists in merely observing that, in the case treated in Section 6 and Appendix V, we dealt already with a most general type of 2nd order fraction including three independent coeffic ients in the numerator. It is obvious that our theorem holds true for any set of these coefficients.

8. *Conclusions.*

(1) A method of computing basic response quantities (normal acceleration at c.g. and at tail, incremental tail loads) in pull-out manoeuvres, based on 'trapezoidal' elevator input, as presented in this report, seems to offer the following advantages:

(i) Simplified analytical approximation to the actual flight manoeuvres;

(ii) In spite of the somewhat complicated derivation, most of the final results (especially peak loads) have been presented in the form of simple explicit formulae;

(iii) A simple discussion in general terms of the effects of all relevant characteristics on the final results is presented in Section 7; the initial 'static' loads are accounted for.

(2) The method is applicable to all tailed elevator-controlled aeroplanes, of arbitrary design and in arbitrary flight conditions, including the full range of speeds well up into supersonic.

(3) A serious limitation of the load factor $n_{\max}$ in cases of flight at high initial C_L, arising from the collapse of lift in the stalling region, has been discussed, and its inclusion in calculation explained.

(4) The final formulae include only a few basic geometrical and aerodynamic data and, in addition, a few overshoot factors. The latter have been reduced to three primary types (E, E', E_1), of which only the first one need be determined for varying duration of the elevator application φ_1, while the two latter ones always pertain to step input ($\varphi_1 = 0$) and need only be multiplied by E to account for the actual value of φ_1. The overshoot factors E and E', important for tail loads, have been charted in extensive ranges (Figs. 5, 6, 10) which, of course, does not preclude the use of exact formulae.

(5) The method seems particularly suitable whenever large ranges of flight conditions (height, speed, c.g. position) must be reckoned with, because the work then reduces to a simple tabulation followed by tracing of a few final curves.

(6) The method may easily be extended to cover asymmetric (rudder induced) manoeuvres.

(7) The method may find additional useful applications in interpreting flight tests.

LIST OF SYMBOLS

a	=	$\partial C_L/\partial\alpha$, lift-curve slope of aeroplane
a_1	=	$\partial C_L'/\partial\alpha'$, lift-curve slope of tailplane
a_2	=	$\partial C_L'/\partial\eta$, rate of change of C_L' with elevator deflection
A, B		Auxiliary symbols, *see* (I.2)
A_1, B_1		Auxiliary symbols, *see* (III.3)
A_2, B_2		Auxiliary symbols, *see* (V.2)
C	=	$\omega + \frac{1}{2}av$, free term of stability quadratic, *see* (2.5)
C_L		Lift coefficient of aeroplane
$\bar{C}_L$		Limiting value of C_L, *see* (7.4)
$C_{L,\,\mathrm{stall}}$		Stalling value of C_L
C_L'		Lift coefficient of tailplane
c		Reference (mean) chord of wing
D	=	$d/d\tau$, differential operator
E		Overshoot factor for normal acceleration at c.g., in case of trapezoidal elevator input, *see* (3.11)
E_0		Overshoot factor for normal acceleration at c.g., in case of step elevator input, *see* (3.5)
E'		Additional overshoot factor for tail incidence, *see* (4.6)
E_1		Additional overshoot factor for tail normal acceleration, *see* (5.7); in Appendix VI, constant term of stability quartic
$F(\varphi)$		Function, auxiliary to determining tail load, *see* (4.30)
H_m		Manoeuvre margin, stick fixed, *see* (4.20) and (2.16)
h		Distance of c.g. aft of L.E. of wing reference chord, expressed as a fraction of this chord
h_0		Distance of aerodynamic centre of wing aft of L.E. of its reference chord, expressed as a fraction of this chord
i_B	=	k_B^2/l^2, inertia coefficient about lateral axis through c.g.
J		Dimensionless angular frequency of short-period oscillation, *see* (2.5)
K_m	=	$-\partial C_m/\partial C_L$, restoring margin, *see* (4.21)
k		Coefficient in 'exponential' formula of Ref. 1, *see* (3.15)
k_B		Radius of gyration of aeroplane about lateral axis through c.g.
l		Tail arm (reference length for pitching moments)
m_q		Dimensionless rotary damping derivative in pitch
$(m_q)_{wb}$		Part of m_q, due to wing and body
m_w		Dimensionless restoring-moment derivative in pitch

$m_{\dot{w}}$ Dimensionless moment derivative in pitch, due to rate of change of w

m_η Dimensionless moment derivative in pitch, due to elevator deflection

n Factor of normal acceleration at c.g. (equal to 'load coefficient minus one'), dimensionless, *see* (2.6)

n_t Coefficient of normal acceleration at tail, *see* (2.10)

n_f = $n_{t,f}$, final (or asymptotic) value of n or n_t when the elevator is held fixed at $\eta = -\eta_f$, *see* (2.11)

$n_{\max}$ First peak value of n in pull-out manoeuvre

$n_{t,0}$ Initial value of n_t

$n_{t,\max}$ First peak value of n_t in pull-out manoeuvre

P Incremental tail load in pull-out manoeuvre

$P_{1\max}$ First maximum incremental tail upload

$P_{2\max}$ Second maximum incremental tail upload, *see* 7.1 (C)

$(-P)_{\max}$ Maximum incremental tail download, *see* (4.31)

P_{tot} Total tail load, including steady and incremental loads

p Auxiliary symbol, *see* (4.28)

q, $\hat{q} = q\hat{t}$ Rate of pitch, in radians per sec, or dimensionless, respectively

R Dimensionless damping factor of short-period oscillation, *see* (2.5)

S, S' Gross wing area, and tailplane area, respectively

t Time in seconds

$\hat{t}$ = $W/g\rho SV$, unit of aerodynamic time, sec

t_1 Value of t at the end of the first part of trapezoidal elevator input, *see* (3.21)

V True speed of aeroplane in undisturbed flight, supposed constant in ordinary pull-out manoeuvres, ft/sec

$\bar{V}$ = $S'l/Sc$, tail volume ratio

W Weight of aeroplane, lb

w, $\hat{w} = w/V$ Normal velocity increment, in ft/sec, or dimensionless, respectively

x, y Auxiliary parameters, *see* (IV.3)

α Incidence of wing, radians

α' Incidence of tailplane, radians

α_{eff}' Effective incidence of tailplane, including effect of rate of pitch and rate of change of w, radians

β = R/J, angular damping index of short-period oscillation

δ Concise pitching-moment derivative due to elevator displacement, dimensionless

ϵ		Angle of downwash, radians
$\Phi(\varphi)$		Function of φ for determining growth of normal acceleration at c.g. in case of trapezoidal elevator input, *see* (3.8) and (3.9)
$\Phi'(\varphi)$		First derivative of $\Phi(\varphi)$; function for determining growth of normal acceleration at c.g. in case of step elevator input, *see* (3.2)
$\Phi''(\varphi)$, $\Phi'''(\varphi)$		Second and third derivatives of $\Phi(\varphi)$
φ	=	$J\tau$, time angle, *see* (3.3)
φ_m		Value of φ for which n reaches its first peak, *see* (3.12)
$\varphi_m{}'$		Value of φ for which $\alpha_{\text{eff}}{}'$ reaches its first peak in case of step elevator input, *see* (4.3)
$\varphi_m{}''$		Value of φ for which $\alpha_{\text{eff}}{}'$ reaches its first peak, in case of trapezoidal elevator input, *see* (4.12)
$\varphi_n{}'$		Value of φ for which n_t reaches its first peak, in case of step elevator input, *see* (5.4)
$\varphi_n{}''$		Value of φ for which n_t reaches its first peak, in case of trapezoidal elevator input, *see* (5.10)
φ_1	=	$J\tau_1$, value of φ at the end of the first part of trapezoidal elevator input
φ^*		Value of φ for which the tail download reaches its true turning value during the first part of trapezoidal elevator input (if existing)
η		Angular deflection of elevator, radians
η_f		Absolute value of η (supposed negative) at which the elevator is finally held in trapezoidal (or exponential) pull-out manoeuvre
ϑ		Phase angle by which maximum tail incidence leads maximum normal acceleration at c.g., *see* (4.3) and (4.12)
ϑ_n		Phase angle by which maximum normal acceleration at tail leads that at c.g., *see* (5.4)
λ		Modifying factor for tail incidence, *see* (2.8)
μ	=	$W/g\rho Sl$, relative density of aeroplane
ν	=	$-m_q/i_B$, concise pitching-moment derivative expressing the effect of rotary damping in pitch, dimensionless
ρ		Air density, slugs/cu. ft
τ	=	$t/\hat{t}$, aerodynamic time, dimensionless
τ_1	=	$t_1/\hat{t}$, value of τ at the end of the first part of trapezoidal elevator input
χ	=	$-m_{\dot{w}}/i_B$, concise pitching-moment derivative expressing the additional damping due to rate of change of w, dimensionless
ω	=	$-\mu m_w/i_B$, concise restoring-moment derivative in pitch, dimensionless

REFERENCES

No.	Author(s)	Title, etc.
1	T. Czaykowski	Loading conditions of tailed aircraft in longitudinal manoeuvres. A.R.C. R. & M. 3001. February, 1955.
2	S. Neumark	Analysis of short-period longitudinal oscillations of an aircraft—interpretation of flight tests. A.R.C. R. & M. 2940. September, 1952.
3	S. Neumark	Operational formulae for response calculations. A.R.C. R. & M. 3075. June, 1956.
4	S. B. Gates	Proposal for an elevator manoeuvrability criterion. A.R.C. R. & M. 2677. June, 1942.
5	H. B. Dickinson	Manoeuvrability and control surface strength criteria for large airplanes. *J. Ae. Sci.*, Vol. 7, No. 11. September, 1940.
6	C. D. Perkins and L. Lees	Manoeuvre loads on horizontal tail surfaces of airplanes. AAF TR. No. 4852. 1942.
7	C. D. Perkins	Non-dimensional chart method for computing the manoeuvre loads on the horizontal tail surfaces of airplanes. AAF TR. No. 4925. 1943.
8	H. A. Pearson	Derivation of charts for determining the horizontal tail load variation with any elevator motion. N.A.C.A. Report 759. 1943.
9	H. A. Pearson, W. A. McGowan and J. J. Donegan	Horizontal tail loads in manoeuvring flight. N.A.C.A. Report 1007. 1951.
10	B. Etkin and F. A. Woodward ..	Calculation of manoeuvring tail loads by the inverse method. N.R.C. of Canada, Aero Report AR–8, Ottawa. 1951.
11	T. Czaykowski	Dynamic fin and rudder loads in yawing manoeuvres. A.R.C. 21,079. June, 1950.
12	D. R. Puttock	The effect of rolling on fin-and-rudder loads in yawing manoeuvres. A.R.C. C.P. 153. January, 1953.
13	D. R. Puttock	Loading conditions following an automatic pilot failure (elevator channel). A.R.C. C.P. 243. February, 1955.
14	D. R. Puttock	Loading conditions following an automatic pilot failure (rudder-channel). A.R.C. C.P. 242. February, 1955.
15	D. R. Puttock	Effects of elevator circuit stiffness on the loading conditions in longitudinal manoeuvres. A.R.C. C.P. 354. March, 1957.
16	A. S. Taylor	The present status of aircraft stability problems in the aero-elastic domain. J. R. Ae. Soc., Vol. 63, pp. 227 to 238. 1959.
17	S. Neumark	Problems of longitudinal stability below minimum drag speed, and theory of stability under constraint. A.R.C. R. & M. 2983. July, 1953.

APPENDIX I

(to Section 3.2)

Details of Calculating Peaks of Normal Acceleration at C.G., Resulting from Trapezoidal Elevator Input

The equation (3.10), representing the growth of the normal acceleration, can be written in the following form, more convenient for differentiation:

$$\frac{n}{n_f} = 1 + \frac{e^{-\beta\varphi}}{\varphi_1(1+\beta^2)}\{A\cos(\varphi-\varphi_1) + B\sin(\varphi-\varphi_1)\}, \tag{I.1}$$

where:

$$\left.\begin{aligned} A &= 2\beta(\cos\varphi_1 - e^{\beta\varphi_1}) - (1-\beta^2)\sin\varphi_1, \\ B &= (1-\beta^2)(e^{\beta\varphi_1} - \cos\varphi_1) - 2\beta\sin\varphi_1. \end{aligned}\right\} \tag{I.2}$$

Differentiating (I.1) with respect to φ, we obtain:

$$\frac{d}{d\varphi}\left(\frac{n}{n_f}\right) = \frac{e^{-\beta\varphi}}{\varphi_1(1+\beta^2)}\{(B-A\beta)\cos(\varphi-\varphi_1) - (A+B\beta)\sin(\varphi-\varphi_1)\}. \tag{I.3}$$

Equating this to zero, we get the following solution for φ_m, determining the positions of all peaks:

$$\tan(\varphi_m-\varphi_1) = \frac{B-A\beta}{A+B\beta} = \frac{e^{\beta\varphi_1} - \cos\varphi_1 - \beta\sin\varphi_1}{\beta\cos\varphi_1 - \beta e^{\beta\varphi_1} - \sin\varphi_1}, \tag{I.4}$$

which is identical with (3.12). We then find:

$$\cos(\varphi_m-\varphi_1) = \pm\frac{A+B\beta}{\sqrt{\{(A^2+B^2)(1+\beta^2)\}}} \quad \sin(\varphi_m-\varphi_1) = \pm\frac{B-A\beta}{\sqrt{\{(A^2+B^2)(1+\beta^2)\}}}, \tag{I.5}$$

where the $\pm$ signs alternate for the consecutive maxima and minima. The first turning value is the absolute maximum, for which the upper signs apply. Substituting (I.5) into (I.1), we obtain:

$$\frac{n_{\max}}{n_f} = 1 + \frac{e^{-\beta\varphi_m}}{\varphi_1(1+\beta^2)}\sqrt{A^2+B^2}\sqrt{1+\beta^2} = 1 + \frac{e^{-\beta\varphi_m}}{\varphi_1}\sqrt{\frac{e^{2\beta\varphi_1} - 2e^{\beta\varphi_1}\cos\varphi_1 + 1}{1+\beta^2}}, \tag{I.6}$$

and this may be conveniently written as (3.11).

The expansions of our formulae in powers of φ_1 have been obtained in the following way. Expanding the numerator and denominator of (I.4), we obtain:

$$\begin{aligned} \tan(\varphi_m-\varphi_1) &= -\frac{\varphi_1}{2}\,\frac{1 + \frac{\beta}{3}\varphi_1 - \frac{1-\beta^2}{12}\varphi_1^2 - \frac{\beta(1-\beta^2)}{60}\varphi_1^3 + \frac{1-\beta^2+\beta^4}{360}\varphi_1^4 + \frac{\beta(1-\beta^2+\beta^4)}{2520}\varphi_1^5\cdots}{1 + \frac{\beta}{2}\varphi_1 - \frac{1-\beta^2}{6}\varphi_1^2 - \frac{\beta(1-\beta^2)}{24}\varphi_1^3 + \frac{1-\beta^2+\beta^4}{120}\varphi_1^4 + \frac{\beta(1-\beta^2+\beta^4)}{720}\varphi_1^5\cdots} \\ &= -\left[\tfrac{1}{2}\varphi_1 - \frac{\beta}{12}\varphi_1^2 + \frac{1}{24}\varphi_1^3 - \frac{\beta(16-\beta^2)}{720}\varphi_1^4 + \frac{6+5\beta^2}{1440}\varphi_1^5 - \frac{\beta(233-16\beta^2+2\beta^4)}{60480}\varphi_1^6\cdots\right] \end{aligned} \tag{I.7}$$

If $\varphi_1 = 0$, then $\varphi_m - \varphi_1 = \pi$, and for small values of φ_1 the angle $(\varphi_m - \varphi_1)$ is somewhat smaller than π. By using the known series for $\tan^{-1}$, we obtain:

$$\varphi_m - \varphi_1 = \pi - \left[\tfrac{1}{2}\varphi_1 - \frac{\beta}{12}\varphi_1^2 - \frac{\beta(1-\beta^2)}{720}\varphi_1^4 - \frac{\beta(3-10\beta^2+3\beta^4)}{90720}\varphi_1^6 \ldots\right], \tag{I.8}$$

and then:

$$e^{-\beta(\varphi_m-\varphi_1)} = e^{-\beta\pi}\left[1 + \frac{\beta}{2}\varphi_1 + \frac{\beta^2}{24}\varphi_1^2 - \frac{\beta^3}{48}\varphi_1^3 - \frac{17\beta^4+8\beta^2}{5760}\varphi_1^4 + \frac{11\beta^5-8\beta^3}{11520}\varphi_1^5 + \right.$$
$$\left. + \frac{485\beta^6+152\beta^4-96\beta^2}{2903040}\varphi_1^6 \ldots\right]. \tag{I.9}$$

Next, we find the expansions:

$$\frac{1-2e^{-\beta\varphi_1}\cos\varphi_1 + e^{-2\beta\varphi_1}}{(1+\beta^2)\varphi_1^2} = 1 - \beta\varphi_1 + \frac{7\beta^2-1}{12}\varphi_1^2 + \frac{\beta-3\beta^3}{12}\varphi_1^3 + \frac{31\beta^4-16\beta^2+1}{360}\varphi_1^4 -$$
$$- \frac{9\beta^5-6\beta^3+\beta}{360}\varphi_1^5 + \frac{127\beta^6-99\beta^4+29\beta^2-1}{20160}\varphi_1^6 \ldots \tag{I.10}$$

and

$$\frac{1}{\varphi_1}\sqrt{\frac{1-2e^{-\beta\varphi_1}\cos\varphi_1 + e^{-2\beta\varphi_1}}{1+\beta^2}} = 1 - \frac{\beta}{2}\varphi_1 + \frac{4\beta^2-1}{24}\varphi_1^2 - \frac{2\beta^3-\beta}{48}\varphi_1^3 + \frac{48\beta^4-28\beta^2+3}{5760}\varphi_1^4 -$$
$$- \frac{16\beta^5-8\beta^3+3\beta}{11520}\varphi_1^5 + \frac{192\beta^6-80\beta^4+80\beta^2-3}{967680}\varphi_1^6 \ldots \tag{I.11}$$

Finally, multiplying the series (I.9) and (I.11), and introducing into (3.11),

$$\frac{n_{\max}}{n_f} - 1 = E = e^{-\beta\pi}\left[1 - \frac{1+\beta^2}{24}\varphi_1^2 + \frac{(1+\beta^2)(3+11\beta^2)}{5760}\varphi_1^4 - \frac{(1+\beta^2)(9-6\beta^2+241\beta^4)}{2903040}\varphi_1^6 \ldots\right] \tag{I.12}$$

which is identical with (3.13). Also, (I.8) is identical with (3.14).

Formulae (3.11) and (3.12) are illustrated in Figs. 5, 6 and 7. Some features of these graphs may be discussed briefly:

(i) Fig. 7 suggests that $(\varphi_m - \varphi_1)$ tends to a certain limit when φ_1 increases indefinitely at constant β. Formula (I.4) shows that this is so, and the limit is given by:

$$\left.\begin{aligned} &\tan(\varphi_m - \varphi_1) \to -\frac{1}{\beta} \\ \text{or} \quad &\varphi_m - \varphi_1 \to \tfrac{1}{2}\pi + \tan^{-1}\beta \end{aligned}\right\} \text{for } \varphi_1 \to \infty \tag{I.13}$$

It is also easily found from (I.4) that the same value is assumed by $(\varphi_m - \varphi_1)$ when $\varphi_1 = \pi$ or 2π or 3π, etc., so that each curve oscillates, with gradually decreasing amplitude, about this asymptotic value. Each curve presents, therefore, an infinite number of turning values, whose exact positions can be found from the equation:

$$e^{-\beta\varphi_1} = \cos\varphi_1 - \beta\sin\varphi_1, \tag{I.14}$$

obtained by equating the first derivative of (I.4) to zero. Substituting (I.14) in (I.4), we obtain:

$$\tan(\varphi_m - \varphi_1) = -\tan\varphi_1, \tag{I.15}$$

as an alternative condition for turning values. It is easily found that the first turning points (minima) of all curves lie on the straight line $\varphi_m - \varphi_1 = 2\pi - \varphi_1$, the second turning points (maxima) on the line $\varphi_m - \varphi_1 = 3\pi - \varphi_1$, and so on, as shown by the broken lines in Fig. 7.

It is also seen that the angle $(\varphi_m - \varphi_1)$ usually lies between $\frac{1}{2}\pi$ and π, and it can only fall below $\frac{1}{2}\pi$ if β is quite small (strictly if β is less than $\sim 0{\cdot}274$), and even then only for some narrow intervals of φ_1.

(ii) Fig. 5 shows that the curves of *overshoot factor* E against φ_1 may oscillate if β is small (the exact limit being a little more than $0{\cdot}2$). The positions of the turning values can be determined by differentiating (I.6) in conjunction with (I.4). This requires some rather complicated algebra but results in a very simple equation:

$$\cosh\beta\varphi_1 - \cos\varphi_1 = \tfrac{1}{2}(1+\beta^2)\varphi_1 \sin\varphi_1 . \tag{I.16}$$

For any given (sufficiently small) β, this equation has a finite number of roots which differ very little from 2π, 3π, 4π, etc.

(iii) *The particular case* $\beta = 0$ is of some interest. All results simplify considerably in this case. The formulae (3.8) and (3.10) become:

$$\left.\begin{aligned} \frac{n}{n_f} &= \frac{\varphi - \sin\varphi}{\varphi_1}, && (0 < \varphi < \varphi_1) \\ \frac{n}{n_f} &= 1 + \frac{\sin(\varphi-\varphi_1) - \sin\varphi}{\varphi_1}, && (\varphi > \varphi_1) \end{aligned}\right\} \tag{I.17}$$

and are illustrated in Fig. 2, for several values of φ_1. Formula (I.4) becomes:

$$\tan(\varphi_m - \varphi_1) = -\tan\frac{\varphi_1}{2}, \tag{I.18}$$

and it is easily found that the graph of (I.18) consists of an infinite number of disconnected straight segments, viz.:

$$\left.\begin{aligned} \varphi_m - \varphi_1 &= \pi - \tfrac{1}{2}\varphi_1 \quad \text{for} \quad 0 < \varphi_1 < 2\pi \\ &= 2\pi - \tfrac{1}{2}\varphi_1 \qquad 2\pi < \varphi_1 < 4\pi \\ &= 3\pi - \tfrac{1}{2}\varphi_1 \qquad 4\pi < \varphi_1 < 6\pi, \text{ etc.} \end{aligned}\right\} \tag{I.19}$$

as shown in Fig. 7.

Finally, the overshoot factor E becomes (*see* 3.11):

$$E = \frac{1}{\varphi_1}\sqrt{(2-2\cos\varphi_1)} = \frac{|\sin\frac{1}{2}\varphi_1|}{\frac{1}{2}\varphi_1}, \tag{I.20}$$

or, expanded:

$$E = 1 - \frac{1}{6}\left(\frac{\varphi_1}{2}\right)^2 + \frac{1}{120}\left(\frac{\varphi_1}{2}\right)^4 - \frac{1}{5040}\left(\frac{\varphi_1}{2}\right)^6 \ldots, \tag{I.21}$$

the latter series being obviously a particular case of (3.13), for $\beta = 0$.

APPENDIX II

(to Section 4.1)

Details of Calculating Peaks of Incremental Incidence of the Tail, Resulting from Step Elevator Input

Differentiating (4.2) with respect to φ, we obtain:

$$\frac{d}{d\varphi}\left(\frac{\alpha_{\text{eff}}'}{\alpha_{\text{eff},f}'}\right) = \Phi''(\varphi) + \lambda\Phi'''(\varphi) = (1+\beta^2)\{\sin\varphi + \lambda(\cos\varphi - \beta\sin\varphi)\}e^{-\beta\varphi}\,. \tag{II.1}$$

Equating this to 0, we get the following expression for φ_m':

$$\tan\varphi_m' = -\frac{\lambda}{1-\beta\lambda}, \tag{II.2}$$

which is equivalent to (4.3) and (4.4).

From (II.2) we obtain:

$$\cos\varphi_m' = -\frac{1-\beta\lambda}{\sqrt{\{1-2\beta\lambda+\lambda^2(1+\beta^2)\}}}, \qquad \sin\varphi_m' = \frac{\lambda}{\sqrt{\{1-2\beta\lambda+\lambda^2(1+\beta^2)\}}} \tag{II.3}$$

and, substituting this into (4.2):

$$\frac{\alpha_{\text{eff},\max}'}{\alpha_{\text{eff},f}'} = 1 + e^{-\beta\varphi_m'}\sqrt{\{1-2\beta\lambda+\lambda^2(1+\beta^2)\}}, \tag{II.4}$$

which is equivalent to (4.5) and (4.6).

The expansions in powers of λ have been obtained as follows. From (4.4) we get:

$$\tan\vartheta = \lambda + \beta\lambda^2 + \beta^2\lambda^3 + \beta^3\lambda^4 + \beta^4\lambda^5 \ldots\,. \tag{II.5}$$

$$\vartheta = \lambda + \beta\lambda^2 + \left(\beta^2 - \frac{1}{3}\right)\lambda^3 + (\beta^3-\beta)\lambda^4 + \left(\beta^4 - 2\beta^2 + \frac{1}{5}\right)\lambda^5 \ldots \tag{II.6}$$

$$e^{\beta\vartheta} = 1 + \beta\lambda + \frac{3}{2}\beta^2\lambda^2 + \left(\frac{13}{6}\beta^3 - \frac{1}{3}\beta\right)\lambda^3 + \left(\frac{73}{24}\beta^4 - \frac{4}{3}\beta^2\right)\lambda^4 + \left(\frac{167}{40}\beta^5 - \frac{7}{2}\beta^3 + \frac{1}{5}\beta\right)\lambda^5 \ldots \tag{II.7}$$

We have also:

$$\sqrt{\{1-2\beta\lambda+\lambda^2(1+\beta^2)\}} = 1 - \beta\lambda + \tfrac{1}{2}\lambda^2 + \tfrac{1}{2}\beta\lambda^3 + \left(\frac{\beta^2}{2} - \frac{1}{8}\right)\lambda^4 + \left(\frac{\beta^3}{2} - \frac{3}{8}\beta\right)\lambda^5 \ldots \tag{II.8}$$

and, multiplying (II.7) by (II.8), we obtain (4.7).

APPENDIX III

(to Section 4.2)

Details of Calculating Peaks of Incremental Incidence of the Tail, Resulting from Trapezoidal Elevator Input

The explicit equivalent of (4.9) is:

$$\frac{\alpha_{\text{eff}}'}{\alpha_{\text{eff},f}'} = \frac{1}{\varphi_1}\left[\varphi - \left(\frac{2\beta}{1+\beta^2} - \lambda\right) + \left\{\left(\frac{2\beta}{1+\beta^2} - \lambda\right)\cos\varphi - \left(\frac{1-\beta^2}{1+\beta^2} + \beta\lambda\right)\sin\varphi\right\} e^{-\beta\varphi}\right] \qquad (0 < \varphi < \varphi_1) \qquad \text{(III.1)}$$

and (4.10) therefore becomes:

$$\frac{\alpha_{\text{eff}}'}{\alpha_{\text{eff},f}'} = 1 + \frac{e^{-\beta\varphi}}{\varphi_1}\{A_1\cos(\varphi-\varphi_1) + B_1\sin(\varphi-\varphi_1)\} \qquad (\varphi > \varphi_1), \qquad \text{(III.2)}$$

where:

$$\left.\begin{aligned} A_1 &= \left(\frac{2\beta}{1+\beta^2} - \lambda\right)\left(\cos\varphi_1 - e^{\beta\varphi_1}\right) - \left(\frac{1-\beta^2}{1+\beta^2} + \beta\lambda\right)\sin\varphi_1, \\ B_1 &= \left(\frac{1-\beta^2}{1+\beta^2} + \beta\lambda\right)\left(e^{\beta\varphi_1} - \cos\varphi_1\right) - \left(\frac{2\beta}{1+\beta^2} - \lambda\right)\sin\varphi_1. \end{aligned}\right\} \qquad \text{(III.3)}$$

The turning values of α_{eff}' occur at a certain $\varphi = \varphi_m''$ which may be obtained by equating the derivative of (III.2) to 0, and the condition for φ_m'' is found, similarly as in Appendix I, in the form:

$$\tan(\varphi_m'' - \varphi_1) = \frac{B_1 - A_1\beta}{A_1 + B_1\beta} = \frac{e^{\beta\varphi_1} - \cos\varphi_1 - \{\beta - \lambda(1+\beta^2)\}\sin\varphi_1}{\{\beta - \lambda(1+\beta^2)\}(\cos\varphi_1 - e^{\beta\varphi_1}) - \sin\varphi_1}. \qquad \text{(III.4)}$$

Comparing now the formulae (3.12) and (4.4) with (III.4), we find easily that the following relationship is identically satisfied:

$$\tan(\varphi_m'' - \varphi_1) = \tan\{(\varphi_m - \varphi_1) - \vartheta\}, \qquad \text{(III.5)}$$

and this is the proof of (4.12). Proceeding further as in Appendix I, we substitute (III.4) into (III.2) and obtain the first turning value (absolute maximum) of the latter in the form:

$$\begin{aligned} \frac{\alpha_{\text{eff},\max}'}{\alpha_{\text{eff},f}'} &= 1 + \frac{e^{-\beta\varphi_m''}}{\varphi_1}\sqrt{\frac{A_1^2 + B_1^2}{1+\beta^2}} = 1 + \frac{e^{-\beta\varphi_m''}}{\varphi_1}\sqrt{\frac{(e^{2\beta\varphi_1} - 2e^{\beta\varphi_1}\cos\varphi_1 + 1)\{1 - 2\beta\lambda + \lambda^2(1+\beta^2)\}}{1+\beta^2}} \\ &= 1 + \frac{e^{-\beta(\varphi_m - \varphi_1)}}{\varphi_1}\sqrt{\frac{1 - 2e^{-\beta\varphi_1}\cos\varphi_1 + e^{-2\beta\varphi_1}}{1+\beta^2}}\, e^{\beta\vartheta}\sqrt{\{1 - 2\beta\lambda + \lambda^2(1+\beta^2)\}} = 1 + EE', \end{aligned} \qquad \text{(III.6)}$$

and thus the formula (4.11) has also been proved.

APPENDIX IV

(to Section 4.4)

Details of Deriving Approximate Formulae for Maximum Download on the Tail (as Worked Out by D. N. Foster)

To determine φ^*, the value of φ for which the function $F(\varphi)$, as given by (4.30), attains its true turning value, the first derivative $F'(\varphi)$ must be equated to 0. We obtain from (4.30):

$$pF'(\varphi) = p - \Phi'(\varphi) - \lambda\Phi''(\varphi) \tag{IV.1}$$

or, substituting for $\Phi'(\varphi)$ from (3.2), and a corresponding expression for $\Phi''(\varphi)$:

$$pF'(\varphi) = p - 1 + [\cos\varphi + \{\beta - \lambda(1+\beta^2)\}\sin\varphi]\, e^{-\beta\varphi}. \tag{IV.2}$$

Making the expression (IV.2) equal to 0 results in a transcendental equation which cannot be solved in a closed form. However, the expression can be expanded into a power series in φ, and then solved by expanding φ into a power series in terms of some of the known parameters (β, λ, p, or some suitable combinations of these parameters which may be treated as small enough to ensure convergence). Many alternative possibilities having been tried, the most promising one seemed to be to *treat the parameters* $\sqrt{p}$ *and* $\lambda/\sqrt{p}$ *as small*† (of the same order), while not making any assumptions as to β. It was found convenient, for simplifying further algebraic work, to introduce auxiliary parameters x and y, defined by:

so that

$$\left.\begin{aligned} 2x &= \sqrt{\frac{2p}{1+\beta^2}} & y &= \lambda\sqrt{\frac{1+\beta^2}{2p}} \\ p &= 2x^2(1+\beta^2) & \lambda &= 2xy \end{aligned}\right\}, \tag{IV.3}$$

and treat x and y as small quantities of the same order. The formula (IV.2) then becomes:

$$2x^2(1+\beta^2)F'(\varphi) = 2x^2(1+\beta^2) - 1 + [\cos\varphi + \{\beta - 2(1+\beta^2)xy\}\sin\varphi]\, e^{-\beta\varphi} \tag{IV.4}$$

or, expanding in powers of φ, and simplifying:

$$\begin{aligned} 2x^2F'(\varphi) = 2x^2 - 2xy\varphi + (4\beta xy - 1)\frac{\varphi^2}{2} + \{\beta - (3\beta^2-1)xy\}\frac{\varphi^3}{3} - \{8\beta(1-\beta^2)xy + (3\beta^2-1)\}\frac{\varphi^4}{24} - \\ - \{2\beta(1-\beta^2) + (1-10\beta^2+5\beta^4)xy\}\frac{\varphi^5}{60} + \{4\beta(3-10\beta^2+3\beta^4)xy - (1-10\beta^2+5\beta^4)\}\frac{\varphi^6}{720}\ldots, \end{aligned} \tag{IV.5}$$

from which expansion it is seen that $F'(\varphi)$ tends to 1 when $\varphi \to 0$, as it should do. Equating (IV.5) to 0, assuming a solution for φ^* as a power series in x and y with indeterminate coefficients, and

† The choice cannot be justified in a strictly mathematical way. The parameter $\sqrt{p}$ may reach values as high as 1 (e.g., $p = 0{\cdot}915$ in the example of Section 6, so that $\sqrt{p} = 0{\cdot}957$); λ is usually quite a small fraction ($0{\cdot}2704$ in our example, but often much smaller for highly loaded modern aeroplanes at great height). The only justification of our choice, for the time being, is that the series seem to converge well.

then working out the coefficients in turn so as to make the coefficients of consecutive powers and products of powers of x and y in the full expression (IV.5) equal to zero, the following solution has been obtained:

$$\varphi^* = 2x\left[1 + \left(\frac{2}{3}\beta x - y\right) + \left(\frac{11\beta^2+3}{18}x^2 + \tfrac{1}{2}y^2\right) + \left(2\beta\frac{43\beta^2+27}{135}x^3 - \frac{4}{3}\beta xy^2\right) + \right.$$
$$\left. + \left(\frac{769\beta^4+786\beta^2+81}{1080}x^4 - \frac{\beta^2+9}{12}x^2y^2 + \frac{4}{3}\beta xy^3 - \frac{1}{8}y^4\right)\ldots\right] \qquad \text{(IV.6)}$$

and this has been verified by direct substitution, the coefficients of all terms up to 6th order having become 0.

The remaining step was to obtain an analogous expansion for $F(\varphi^*)$, the turning value itself. Integrating (IV.5) gives:

$$2x^2F(\varphi) = 2x^2\varphi - xy\varphi^2 + (4\beta xy - 1)\frac{\varphi^3}{6} + \{\beta - (3\beta^2-1)xy\}\frac{\varphi^4}{12} - \left\{8\beta(1-\beta^2)xy + (3\beta^2-1)\right\}\frac{\varphi^5}{120} -$$
$$- \{2\beta(1-\beta^2) + (1-10\beta^2+5\beta^4)xy\}\frac{\varphi^6}{360} +$$
$$+ \{4\beta(3-10\beta^2+3\beta^4)xy - (1-10\beta^2+5\beta^4)\}\frac{\varphi^7}{5040}\ldots, \qquad \text{(IV.7)}$$

the constant being $= 0$, as $F(0) = 0$. Finally, substituting (IV.6) into (IV.7), and simplifying, the result has been obtained:

$$F_{\max} = F(\varphi^*) = \frac{4}{3}x\left[1 + \left(\frac{\beta}{2}x - \frac{3}{2}y\right) + \left(\frac{11\beta^2+3}{30}x^2 + \frac{3}{2}y^2\right) + \left(\frac{43\beta^2+27}{135}\beta x^3 - 2\beta xy^2 - y^3\right) + \right.$$
$$\left. + \left(\frac{769\beta^4+786\beta^2+81}{2520}x^4 - \frac{\beta^2+9}{12}x^2y^2 + 4\beta xy^3 + \frac{3}{8}y^4\right)\ldots\right]. \qquad \text{(IV.8)}$$

The solutions (IV.6) and (IV.8) can be rewritten by using (IV.3) in terms of the original parameters p and λ. It will suffice to write only a few initial terms of both series:

$$\left.\begin{aligned}
\varphi^* &= \sqrt{\frac{2p}{1+\beta^2}}\left[1 + \left(\frac{\beta}{3}\sqrt{\frac{2p}{1+\beta^2}} - \lambda\sqrt{\frac{1+\beta^2}{2p}}\right) + \left\{\frac{11\beta^2+3}{36(1+\beta^2)}p + \frac{1+\beta^2}{4}\frac{\lambda^2}{p}\right\} + \ldots\right], \\
F_{\max} &= F(\varphi^*) = \frac{2}{3}\sqrt{\frac{2p}{1+\beta^2}}\left[1 + \left(\frac{\beta}{4}\sqrt{\frac{2p}{1+\beta^2}} - \frac{3}{2}\lambda\sqrt{\frac{1+\beta^2}{2p}}\right) + \right. \\
&\quad \left. + \left\{\frac{11\beta^2+3}{60(1+\beta^2)}p + \frac{3(1+\beta^2)}{4}\frac{\lambda^2}{p}\right\} + \ldots\right].
\end{aligned}\right\} \text{(IV.9)}$$

The very rough approximations (4.35) are obtained by keeping only the first terms in each of the series (IV.9).

APPENDIX V

(to Section 5)

Details of Calculating Normal Acceleration at Tail, Especially its Peaks, Resulting from Step or Trapezoidal Elevator Input

(A) *Step elevator input.*

The equation (5.2) may be written:

$$\frac{n_t}{n_f} = 1 - (A_2 \cos\varphi + B_2 \sin\varphi) e^{-\beta\varphi}, \tag{V.1}$$

where:

$$A_2 = 1 + \frac{2C}{\mu a}, \qquad B_2 = \beta\left(1 + \frac{2C}{\mu a}\right) - \frac{C(4R-a)}{\mu a J}. \tag{V.2}$$

The condition for peaks of n_t becomes:

$$\tan\varphi_n{}' = \frac{B_2 - A_2\beta}{A_2 + B_2\beta} = -\frac{J(4R-a)}{\mu a + 2C - R(4R-a)} \tag{V.3}$$

which, for the first peaks, is identical with (5.4) and (5.5). The absolute maximum is:

$$\frac{n_{t,\max}}{n_f} = 1 + e^{-\beta\varphi_n'}\sqrt{\frac{A_2{}^2 + B_2{}^2}{1+\beta^2}} = 1 + e^{-\beta\varphi_n'}\sqrt{\left\{\left(1 + \frac{2C}{\mu a}\right)^2 - \left(\frac{2R}{\mu} + \frac{C}{\mu^2}\right)\left(\frac{4R}{a} - 1\right)\right\}}, \tag{V.4}$$

which is identical with (5.6) and (5.7).

The expansion of E_1 into a power series is obtained as follows. From (5.5) we find:

$$\tan\vartheta_n = \frac{J(4R-a)}{\mu a} - \frac{J(4R-a)\{2C - R(4R-a)\}}{\mu^2 a^2} + \frac{J(4R-a)\{2C - R(4R-a)\}^2}{\mu^3 a^3} \tag{V.5}$$

hence:

$$\vartheta_n = \frac{J(4R-a)}{\mu a} - \frac{J(4R-a)\{2C - R(4R-a)\}}{\mu^2 a^2} + \\ + \frac{J(4R-a)\{2C - R(4R-a)\}^2 - \frac{1}{3}J^3(4R-a)^3}{\mu^3 a^3} \cdots, \tag{V.6}$$

and

$$e^{\beta\vartheta_n} = 1 + \frac{R(4R-a)}{\mu a} + \frac{\frac{3}{2}R^2(4R-a)^2 - 2RC(4R-a)}{\mu^2 a^2} + \\ + \frac{2R(4R-a)\{2C - R(4R-a)\}\{C - R(4R-a)\} - \frac{1}{6}R(4R-a)^3(2C - 3R^2)}{\mu^3 a^3} \cdots \tag{V.7}$$

Similarly, expanding the square root in (5.7), we obtain:

$$\sqrt{\left\{1 + \frac{4C - 2R(4R-a)}{\mu a} + \frac{4C^2 - aC(4R-a)}{\mu^2 a^2}\right\}} = 1 + \frac{2C - R(4R-a)}{\mu a} + \frac{\frac{1}{2}J^2(4R-a)^2}{\mu^2 a^2} - \\ - \frac{J^2(4R-a)^2\{C - \frac{1}{2}R(4R-a)\}}{\mu^3 a^3} \cdots \tag{V.8}$$

and, multiplying (V.7) by (V.8), we get finally (5.8).

(B) *Trapezoidal elevator input.*

For the 1st part of the manoeuvre, from (2.15) and (3.6):

$$\frac{n_t}{n_f} = \frac{JC\left(1-\frac{D}{\mu}-\frac{2}{\mu a}D^2\right)}{\varphi_1 D(D^2+2RD+C)}, \tag{V.9}$$

and the functional solution (Ref. 3, form. 111) becomes:

$$\begin{aligned}\frac{n_t}{n_f} &= \frac{1}{\varphi_1}\left\{\Phi(\varphi)-\frac{J}{\mu}\Phi'(\varphi)-\frac{2J^2}{\mu a}\Phi''(\varphi)\right\} \\ &= \frac{1}{\varphi_1}\left[\varphi-\left(\frac{J}{\mu}+\frac{2\beta}{1+\beta^2}\right)+\left\{\left(\frac{J}{\mu}+\frac{2\beta}{1+\beta^2}\right)\cos\varphi-\left(\frac{2C}{\mu a}-\frac{R}{\mu}+\frac{1-\beta^2}{1+\beta^2}\right)\sin\varphi\right\}e^{-\beta\varphi}\right].\end{aligned} \tag{V.10}$$

During the 2nd part of the manoeuvre, we have:

$$\frac{n_t}{n_f} = \frac{1}{\varphi_1}\left[\Phi(\varphi)-\Phi(\varphi-\varphi_1)-\frac{J}{\mu}\{\Phi'(\varphi)-\Phi'(\varphi-\varphi_1)\}-\frac{2J^2}{\mu a}\{\Phi''(\varphi)-\Phi''(\varphi-\varphi_1)\}\right. \tag{V.11}$$

or

$$\frac{n_t}{n_f} = 1+\frac{e^{-\beta\varphi}}{\varphi_1}\{A_3\cos(\varphi-\varphi_1)+B_3\cos(\varphi-\varphi_1)\}, \tag{V.12}$$

where

$$\left.\begin{aligned}A_3 &= \left(\frac{J}{\mu}+\frac{2\beta}{1+\beta^2}\right)\left(\cos\varphi_1-e^{\beta\varphi_1}\right)-\left(\frac{2C}{\mu a}-\frac{R}{\mu}+\frac{1-\beta^2}{1+\beta^2}\right)\sin\varphi_1, \\ B_3 &= \left(\frac{2C}{\mu a}-\frac{R}{\mu}+\frac{1-\beta^2}{1+\beta^2}\right)\left(e^{\beta\varphi_1}-\cos\varphi_1\right)-\left(\frac{J}{\mu}+\frac{2\beta}{1+\beta^2}\right)\sin\varphi_1.\end{aligned}\right\} \tag{V.13}$$

The first (positive) peak is obtained for $\varphi = \varphi_n''$, where:

$$\tan(\varphi_n''-\varphi_1) = \frac{B_3-A_3\beta}{A_3+B_3\beta} = \frac{\left(1+\frac{2C}{\mu a}\right)\left(e^{\beta\varphi_1}-\cos\varphi_1\right)-\left(\beta+J\frac{1+\beta^2}{\mu}-\frac{2\beta C}{\mu a}\right)\sin\varphi_1}{\left(\beta+J\frac{1+\beta^2}{\mu}-\frac{2\beta C}{\mu a}\right)\left(\cos\varphi_1-e^{\beta\varphi_1}\right)-\left(1+\frac{2C}{\mu a}\right)\sin\varphi_1}, \tag{V.14}$$

and it may be noticed that this becomes identical with (I.4) when terms containing μ in the denominator are omitted, and identical with (V.3) when $\varphi_1 \to 0$. It is also easily found, comparing (V.14) with (I.4) and (5.5), that

$$\tan(\varphi_n''-\varphi_1) = \tan\{(\varphi_m-\varphi_1)-\vartheta_n\}, \tag{V.15}$$

which is the proof of (5.10). Proceeding further as in Appendix III, we substitute (V.14) into (V.12), and obtain:

$$\begin{aligned}\frac{n_{t,\max}}{n_f} &= 1+\frac{e^{-\beta\varphi_n''}}{\varphi_1}\sqrt{\frac{A_3^2+B_3^2}{1+\beta^2}} = 1+\frac{e^{-\beta\varphi_n''}}{\varphi_1}\sqrt{\frac{e^{2\beta\varphi_1}-2e^{\beta\varphi_1}\cos\varphi_1+1}{1+\beta^2}}\times \\ &\qquad\times\sqrt{\left(1+\frac{2C}{\mu a}\right)^2-\left(\frac{2R}{\mu}+\frac{C}{\mu^2}\right)\left(\frac{4R}{a}-1\right)} \\ &= 1+\frac{e^{-\beta(\vartheta_m-\varphi_1)}}{\varphi_1}\sqrt{\frac{1-2e^{-\beta\varphi_1}\cos\varphi_1+e^{-2\beta\varphi_1}}{1+\beta^2}}\times \\ &\qquad\times e^{\beta\vartheta_n}\sqrt{\left\{\left(1+\frac{2C}{\mu a}\right)^2-\left(\frac{2R}{\mu}+\frac{C}{\mu^2}\right)\left(\frac{4R}{a}-1\right)\right\}} = 1+EE_1,\end{aligned} \tag{V.16}$$

and thus the formula (5.9) has also been proved.

APPENDIX VI

(to Section 7.3)

Effects of Varying Forward Speed on Tail Load

If the elevator is kept deflected for a long time, it will not be permissible to assume the forward speed as constant, and the equations of motion {(2.1), (2.2)} will have to be replaced by a more complicated system of the fourth order which can be found, for instance, in Ref. 2 {equations (I.16)}. The complete solutions for the variables $\hat{u}$, $\hat{w}$, $\hat{q}$ may be found as shown in Ref. 2, and hence the formulae for tail incidence and tail load may also be determined. These solutions contain, in addition to short-period terms, also phugoid oscillatory terms, and are rather complicated. The only interesting point, however, is their asymptotic behaviour after a very long time (assuming that $\eta = \text{const.} = -\eta_f$), and this can be determined quite easily, as shown in Ref. 17, equations (3.3). We have:

$$\hat{u}_{\text{as}} = \frac{C_L z_w \delta\eta_f}{2E_1}, \quad \hat{w}_{\text{as}} = -\frac{C_L z_u \delta\eta_f}{2E_1}, \quad \hat{q}_{\text{as}} = 0, \tag{VI.1}$$

where

$$\left.\begin{aligned} z_w &= -\tfrac{1}{2}(a + C_D) \approx -\tfrac{1}{2}a, \\ z_u &= -C_L \text{ (neglecting compressibility effects)}, \end{aligned}\right\} \tag{VI.2}$$

and E_1, the constant term of the stability quartic, is given by:

$$E_1 = \frac{\mu}{i_B}\frac{c}{4l} C_L^2 a K_n, \tag{VI.3}$$

K_n being the *static margin*. It may be noticed that the asymptotic value of the normal-acceleration factor n will be 0 because, in this case:

$$n = -\frac{2}{C_L}(z_u\hat{u} + z_w\hat{w}), \tag{VI.4}$$

and hence, substituting (VI.1), we obtain $n_{\text{as}} = 0$. This means that the asymptotic conditions represent a new steady rectilinear flight, at a higher incidence and lower speed.

Taking into account the expression for δ from (2.16), the formulae (VI.1) become:

$$\hat{u}_{\text{as}} = -\frac{a_2 \overline{V} \eta_f}{2C_L K_n} \tag{VI.5}$$

$$\hat{w}_{\text{as}} = \frac{a_2 \overline{V} \eta_f}{a K_n}. \tag{VI.6}$$

The incremental tail incidence in asymptotic conditions will be $\hat{w}_{\text{as}}\,(1 - d\epsilon/d\alpha)$, and hence the incremental tail load in these conditions, from (4.13) and (VI.6):

$$P_{\text{as}} = \tfrac{1}{2}\rho V^2 (1 + \hat{u}_{\text{as}})^2 S' a_2 \eta_f \left\{ \frac{a_1 \overline{V}\left(1 - \dfrac{d\epsilon}{d\alpha}\right)}{a K_n} - 1 \right\}, \tag{VI.7}$$

the factor $(1 + \hat{u}_{\text{as}})^2$ being introduced to account for the reduction of speed. Strictly speaking, this factor should be neglected if we were to follow rigidly the linear theory. If, however, the elevator deflection η_f is considerable (as it must be to produce large $n_{\max}$), then $\hat{u}_{\text{as}}$ may assume large negative values, and it would be unreasonable to neglect this alleviation.

The first maximum tail upload is, according to (4.15):

$$P_{1\max} = \tfrac{1}{2}\rho V^2 S' a_2 \eta_f \left\{ \frac{a_1 \overline{V} \left(1 - \frac{d\epsilon}{d\alpha} + \frac{a}{2\mu}\right)\left(1 + EE'\right)}{aH_m} - 1 \right\}, \tag{VI.8}$$

and it is seen that formulae (VI.7) and (VI.8) are very similar. The presence of the factor $(1+\hat{u}_{as})^2$ and absence of $a/2\mu$ and EE' in (VI.7) all contribute to make P_{as} smaller than $P_{1\max}$, but a considerable difference may result from the manoeuvre margin H_m being replaced by the static margin K_n. The latter can assume widely different values in various flight conditions. If $K_n > H_m$, as it should be in most cases, then P_{as} will certainly be considerably smaller than $P_{1\max}$. However, a great caution is advisable when using the formula (VI.7) even if $K_n > H_m$, and more so if $K_n < H_m$, because the entire linear theory may very often break down. To show this, we notice, from (2.18) and (4.17):

$$\hat{w}_{\max} = \frac{a_2 \overline{V} \eta_f (1+E)}{C_L H_m}, \qquad n_{\max} = \frac{a_2 \overline{V} \eta_f (1+E)}{aH_m}, \tag{VI.9}$$

and therefore (VI.5) and (VI.6) may be written:

$$\hat{u}_{as} = -\frac{n_{\max}}{2(1+E)} \frac{H_m}{K_n}, \tag{VI.10}$$

$$\hat{w}_{as} = \frac{\hat{w}_{\max}}{1+E} \frac{H_m}{K_n}. \tag{VI.11}$$

If $n_{\max}$ has usual large values, and if K_n is not many times greater than H_m, the formula (VI.10) will give absurdly large negative values for $\hat{u}_{as}$, often numerically greater than 1. This means that the linear theory (based on the assumption that $\hat{u}$ and $\hat{w}$ are both small fractions) breaks down before the asymptotic conditions are reached, or that the asymptotic conditions do not exist. This is also seen from (VI.11) which shows that the incremental incidence $\hat{w}_{as}$ may become very large. Obviously, if the elevator deflection is sufficient to produce large $n_{\max}$ in the early stage of the pull-out manoeuvre, and if the elevator is kept so deflected for a long time, then either the aeroplane will stall or, at least, will reach a new equilibrium at a very large C_L and greatly reduced speed. In neither case will the above formulae for asymptotic conditions apply, and the correct procedure will be to try to find the speed, incidence and tail load from static-equilibrium conditions, taking into account true (not linearised) polar and trim curves. It is highly improbable that such a procedure could lead to greater tail loads than those obtaining in high-speed manoeuvres.

It is clear from the above discussion that the formulae for asymptotic conditions can only be applied for sufficiently small elevator deflections, and even so only if the static margin K_n is positive and not too small. Should K_n become 0 or negative, the aeroplane would be statically unstable and a steady elevator deflection would lead to divergence, and could not be maintained for any length of time.

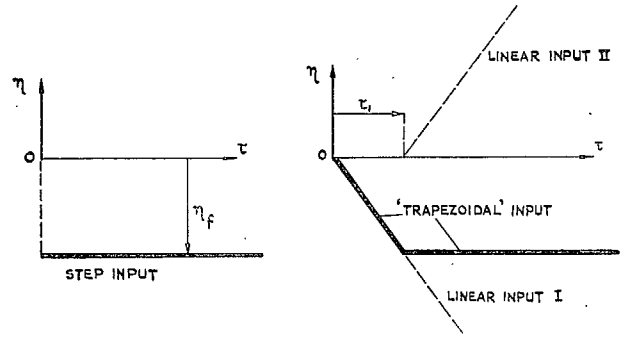

FIG. 1. Elevator step input, and trapezoidal input.

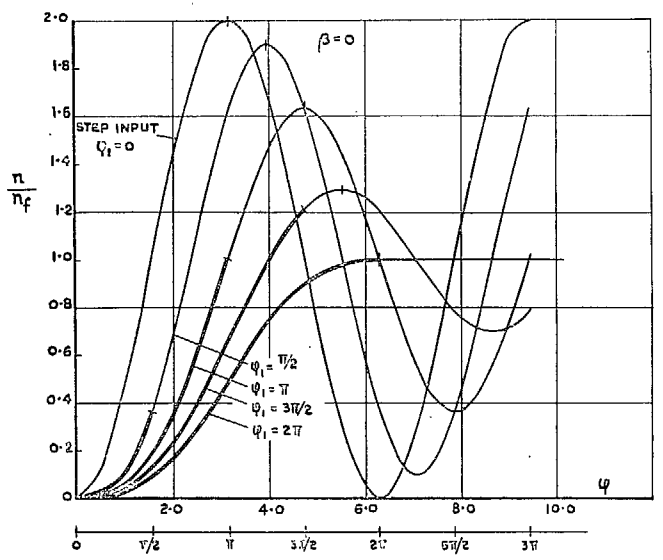

FIG. 2. Trapezoidal input. Growth of normal acceleration at c.g. for varying time angle, φ_1, of input application; angular damping index $\beta = 0$.

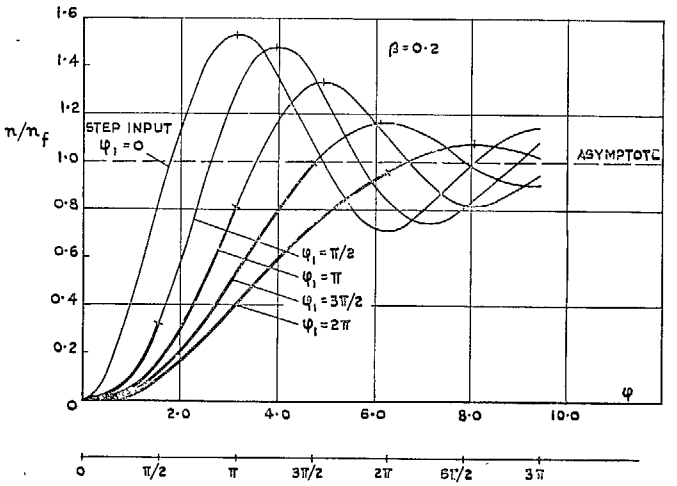

FIG. 3. Trapezoidal input. Growth of normal acceleration at c.g. for varying time angle, φ_1, of input application; angular damping index $\beta = 0{\cdot}2$.

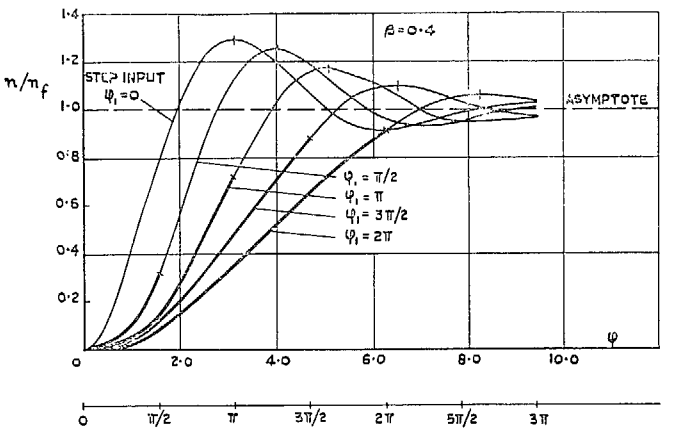

FIG. 4. Trapezoidal input. Growth of normal acceleration at c.g. for varying time angle, φ_1, of input application; angular damping index $\beta = 0{\cdot}4$.

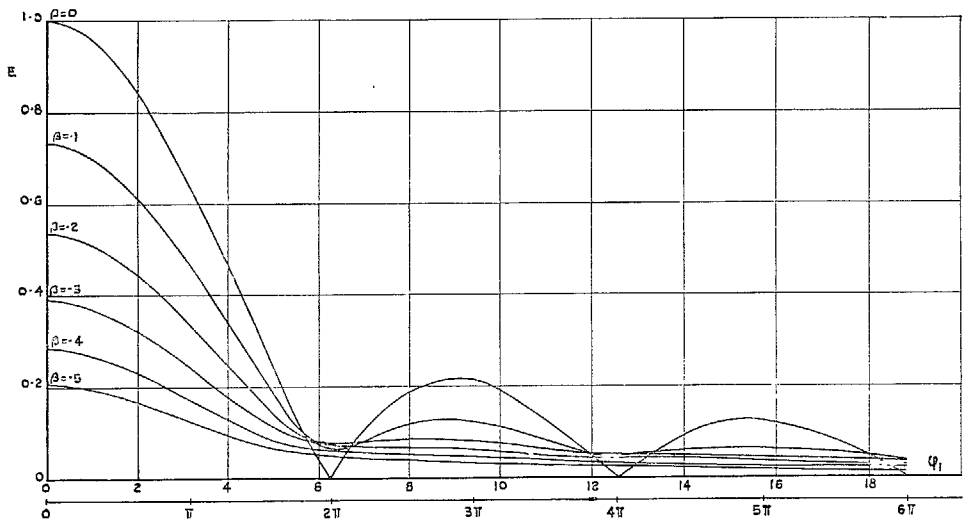

FIG. 5. Overshoot factor, E, of normal acceleration at c.g. for varying β and φ_1. Comprehensive diagram for a wide range of φ_1. Trapezoidal input.

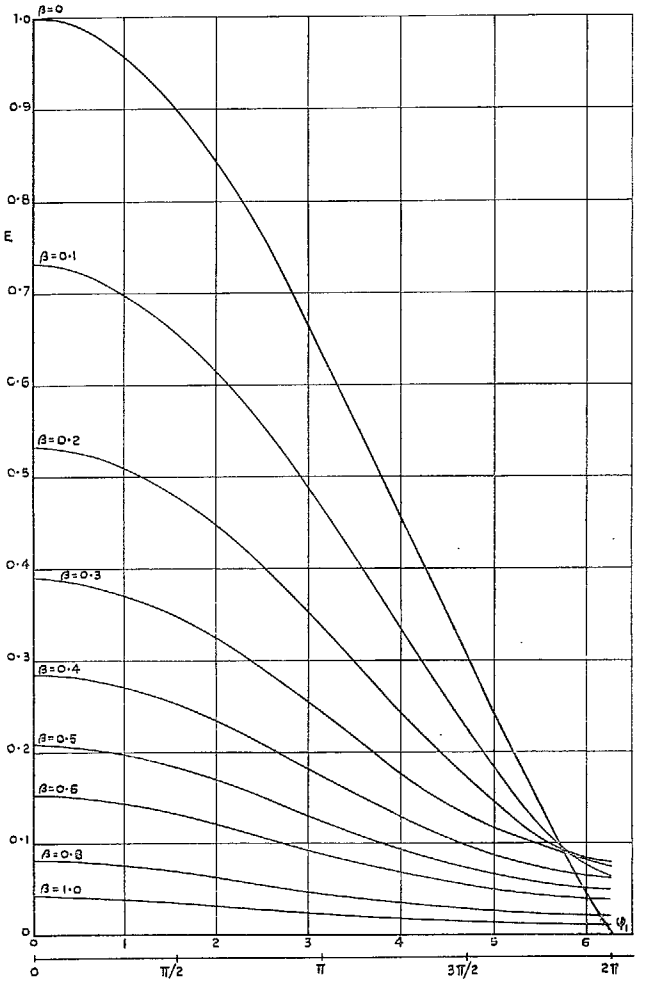

FIG. 6. Overshoot factor, E, for varying β and φ_1. Large-scale diagram for a small range of φ_1. Trapezoidal input.

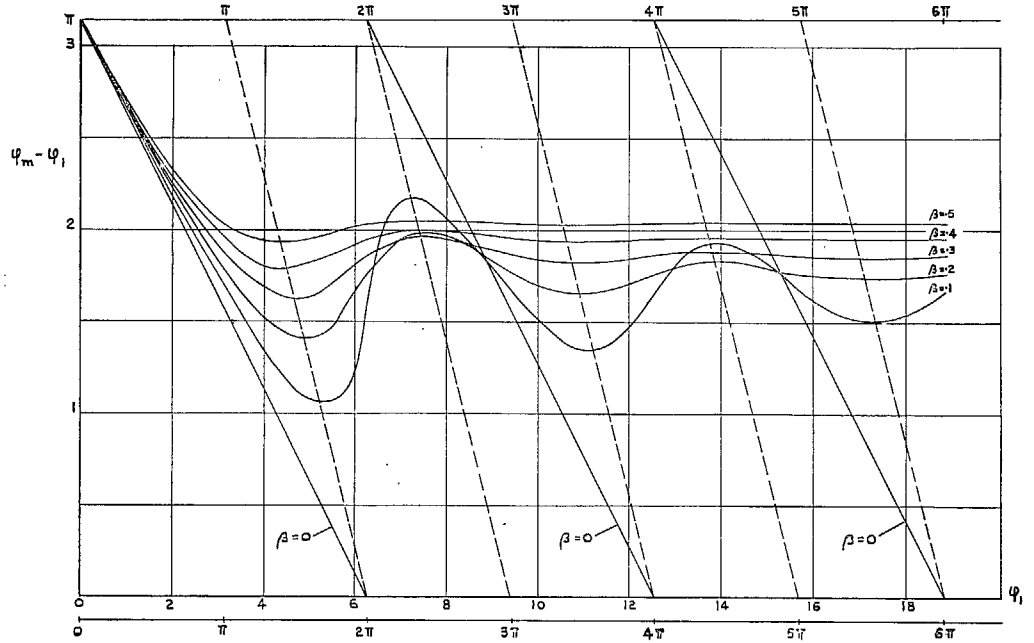

FIG. 7. Time angle $(\varphi_m - \varphi_1)$ by which peak of normal acceleration at c.g. follows end of input. Trapezoidal input, varying β and φ_1.

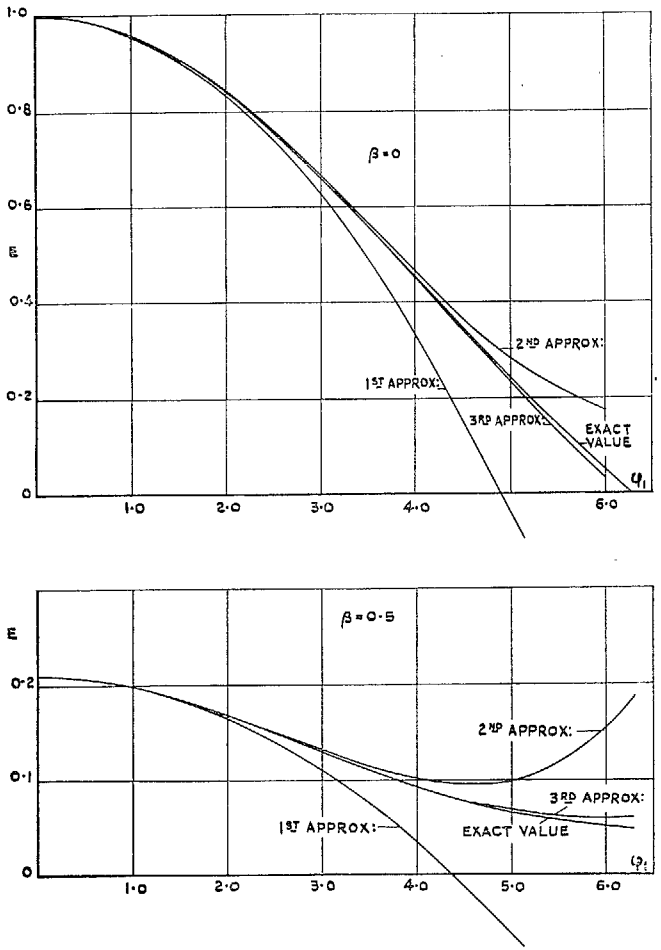

FIG. 8. Comparison of approximate values of overshoot factor, E, from series expansion with exact values, for varying φ_1; $\beta = 0$ and $0 \cdot 5$.

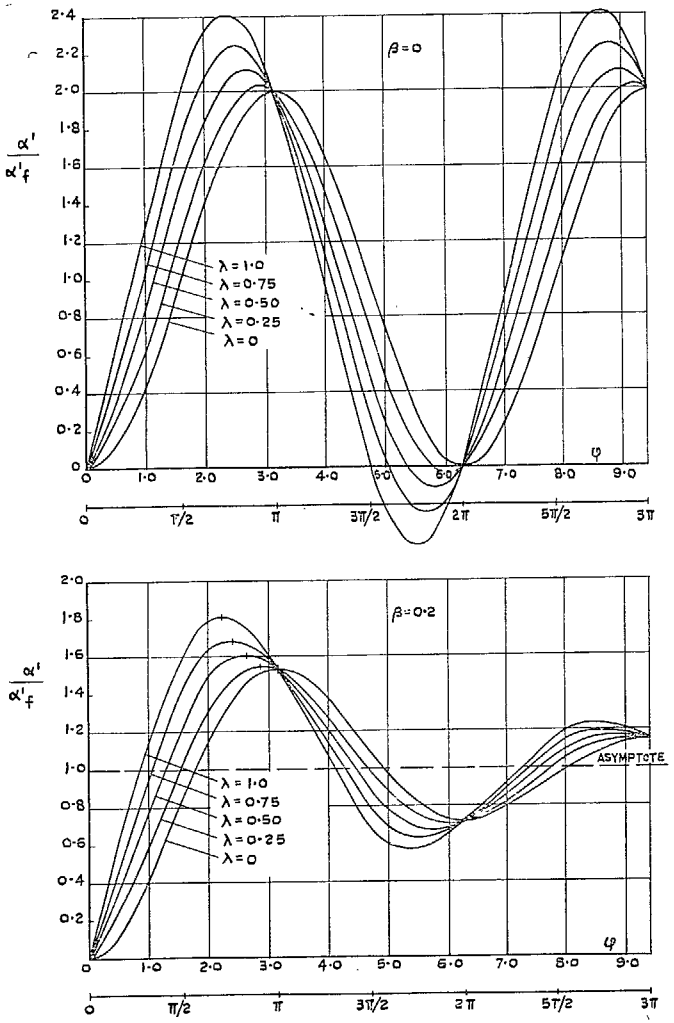

FIG. 9. Growth of incremental tail incidence resulting from step elevator input, for several values of modifying factor λ; $\beta = 0$ and $0 \cdot 2$.

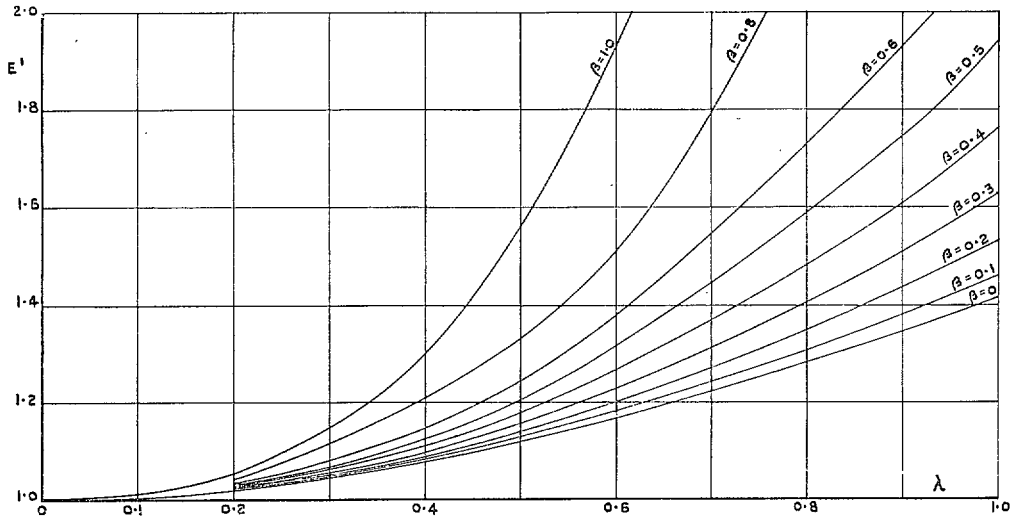

FIG. 10. Additional overshoot factor, E', for tail incidence, for varying λ and β.

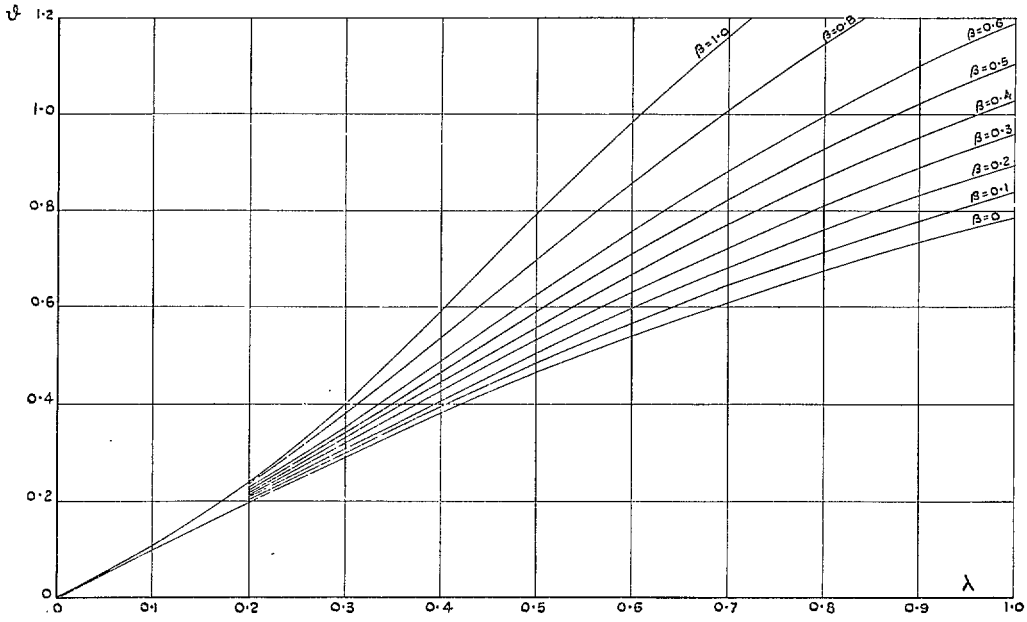

FIG. 11. Time angle ϑ by which peak of tail incidence leads maximum normal acceleration at c.g., for varying λ and β.

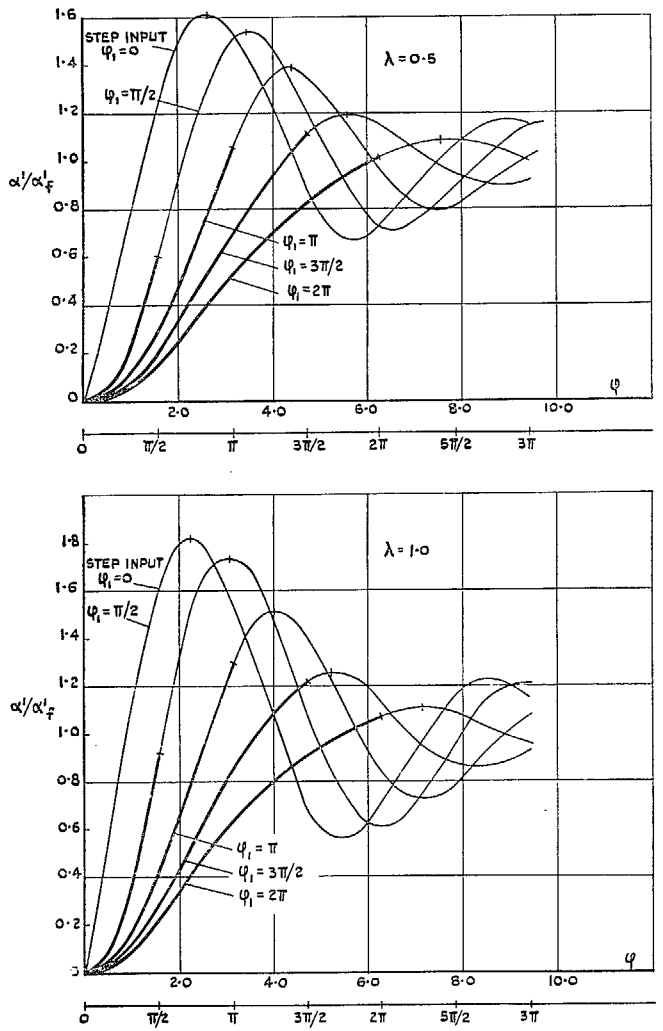

FIG. 12. Growth of incremental tail incidence resulting from trapezoidal elevator input, for varying φ_1; $\beta = 0{\cdot}2$; $\lambda = 0{\cdot}5$ and $1{\cdot}0$.

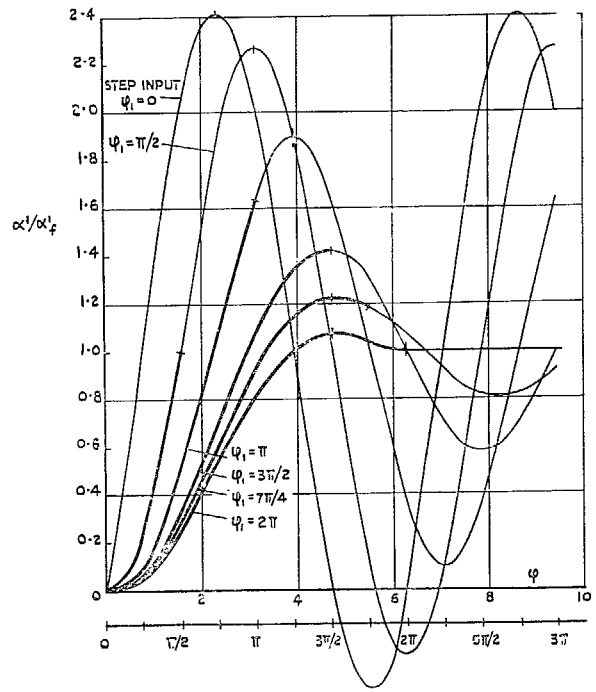

FIG. 13. Growth of incremental tail incidence resulting from trapezoidal elevator input, for varying φ_1; $\beta = 0$; $\lambda = 1{\cdot}0$.

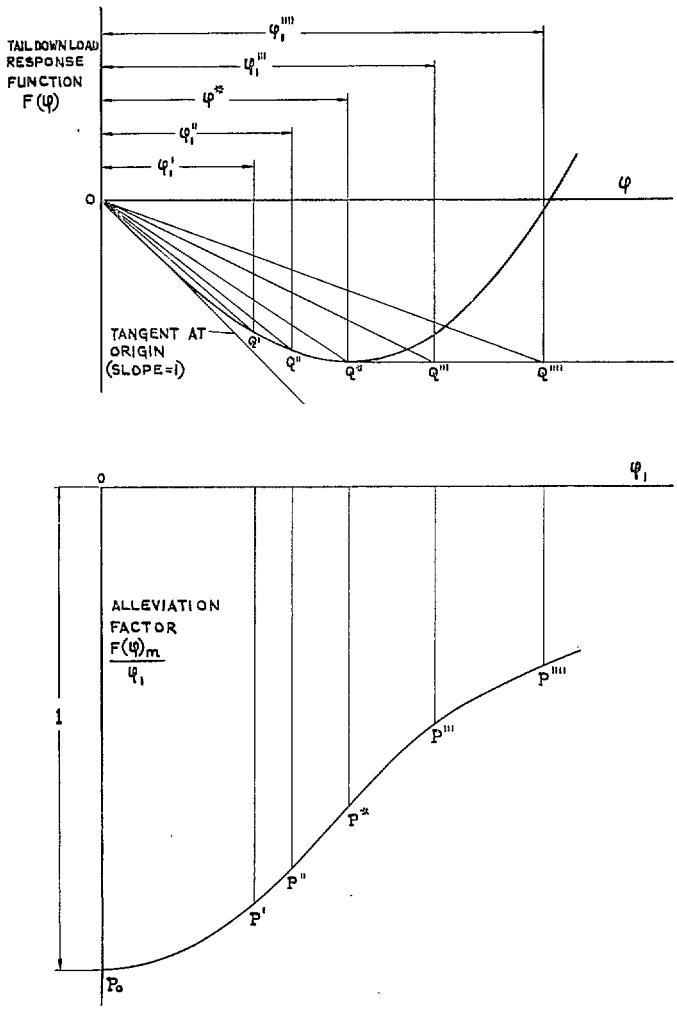

FIG. 14. Explanatory to determining maximum download on tail. (*See* Section 4.4.)

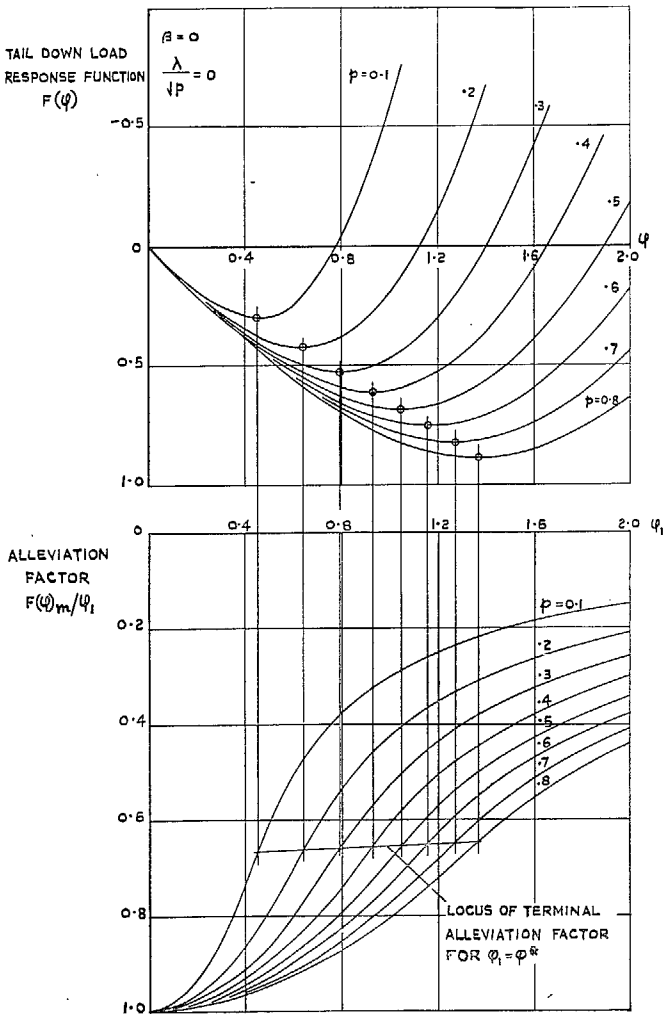

FIG. 15. Graphs of $F(\varphi)$ and $F(\varphi)_m/\varphi_1$ for determining maximum tail downloads and checking series expansions. $\beta = 0$, $\lambda = 0$, variable p. (*See* Section 4.4.)

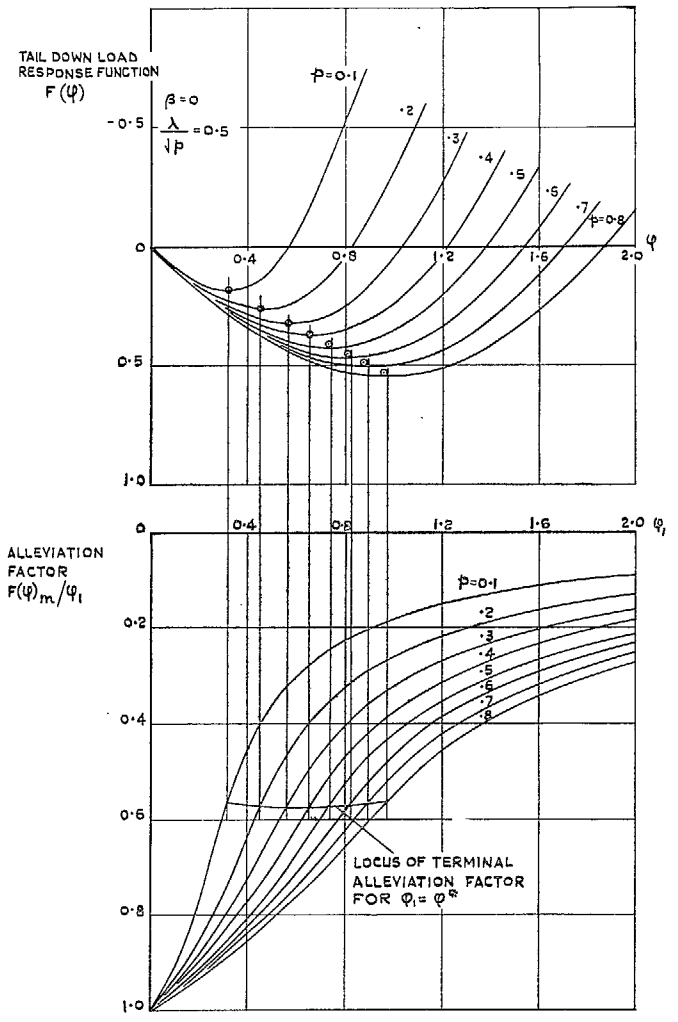

FIG. 16. Graphs of $F(\varphi)$ and $F(\varphi)_m/\varphi_1$ for determining maximum tail downloads and checking series expansions. $\beta = 0$, $\lambda/\sqrt{p} = 0{\cdot}5$, variable p. (*See* Section 4.4.)

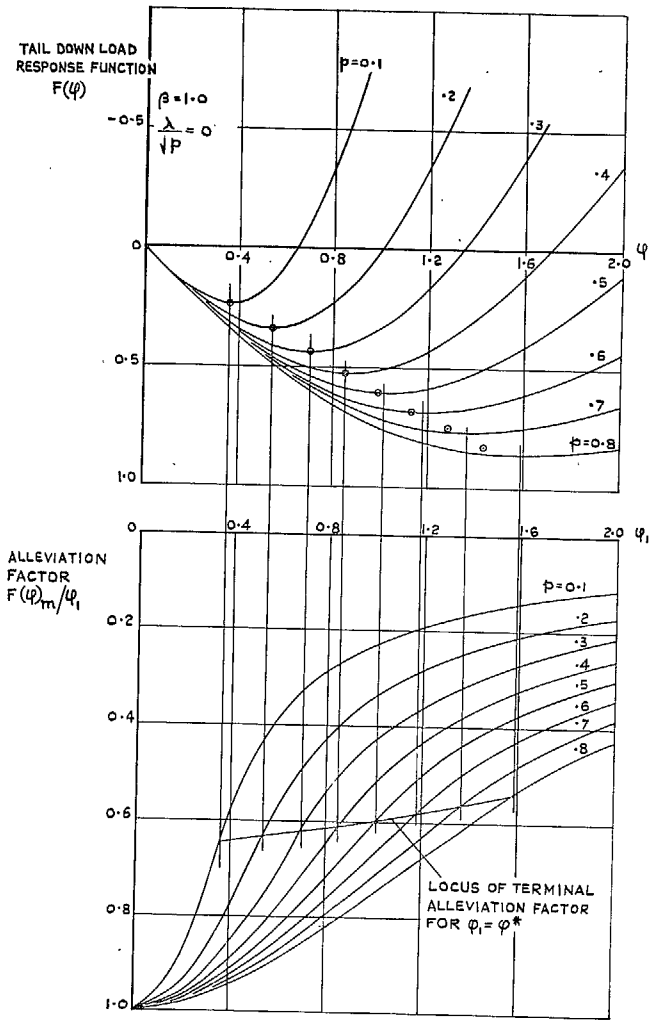

FIG. 17. Graphs of $F(\varphi)$ and $F(\varphi)_m/\varphi_1$ for determining maximum tail downloads and checking series expansions. $\beta = 1{\cdot}0$, $\lambda = 0$, variable p. (*See* Section 4.4.)

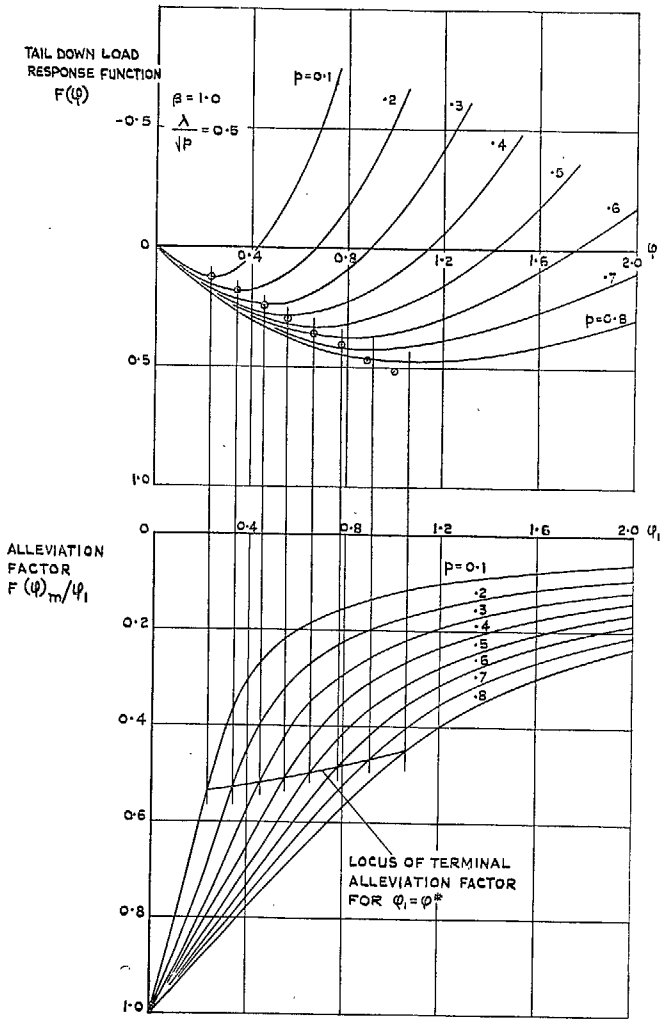

FIG. 18. Graphs of $F(\varphi)$ and $F(\varphi)_m/\varphi_1$ for determining tail loads and checking series expansions. $\beta = 1{\cdot}0$, $\lambda/\sqrt{p} = 0{\cdot}5$, variable p. (*See* Section 4.4.)

(87292) Wt. 1857/64 K.5 7/63 Hw.

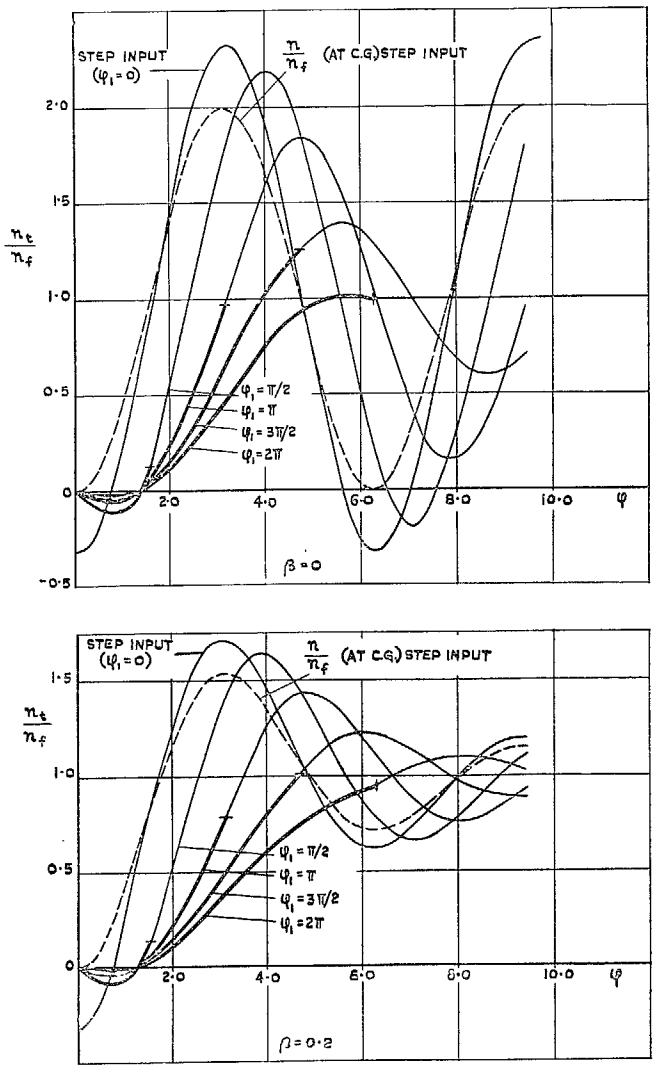

FIG. 19. Growth of normal acceleration at tail, for varying φ_1; $\beta = 0$ and $0{\cdot}2$, $J/\mu = 0{\cdot}08$, $J/a = 2{\cdot}0$.

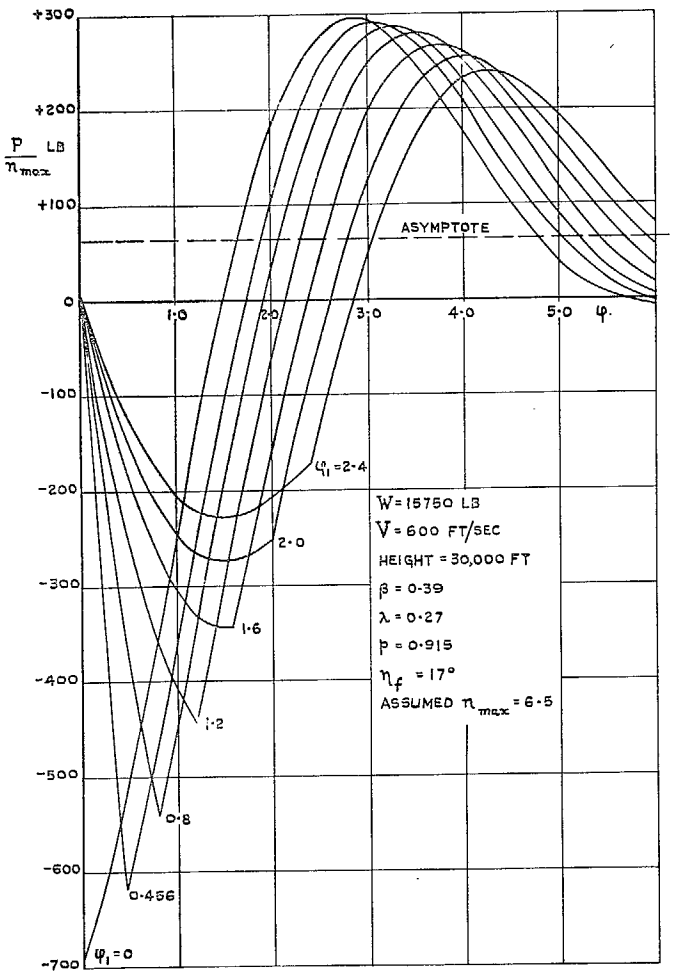

FIG. 20. Illustration of numerical example (Section 6). Variation of tail load, for varying φ_1.

Publications of the Aeronautical Research Council

ANNUAL TECHNICAL REPORTS OF THE AERONAUTICAL RESEARCH COUNCIL (BOUND VOLUMES)

1942 Vol. I. Aero and Hydrodynamics, Aerofoils, Airscrews, Engines. 75*s.* (post 2*s.* 9*d.*)
Vol. II. Noise, Parachutes, Stability and Control, Structures, Vibration, Wind Tunnels, 47*s.* 6*d.* (post 2*s.* 3*d.*)

1943 Vol. I. Aerodynamics, Aerofoils, Airscrews. 80*s.* (post 2*s.* 6*d.*)
Vol. II. Engines, Flutter, Materials, Parachutes, Performance, Stability and Control, Structures. 90*s.* (post 2*s.* 9*d.*)

1944 Vol. I. Aero and Hydrodynamics, Aerofoils, Aircraft, Airscrews, Controls. 84*s.* (post 3*s.*)
Vol. II. Flutter and Vibration, Materials, Miscellaneous, Navigation, Parachutes, Performance, Plates and Panels, Stability, Structures, Test Equipment, Wind Tunnels. 84*s.* (post 3*s.*)

1945 Vol. I. Aero and Hydrodynamics, Aerofoils. 130*s.* (post 3*s.* 6*d.*)
Vol. II. Aircraft, Airscrews, Controls. 130*s.* (post 3*s.* 6*d.*)
Vol. III. Flutter and Vibration, Instruments, Miscellaneous, Parachutes, Plates and Panels, Propulsion. 130*s.* (post 3*s.* 3*d.*)
Vol. IV. Stability, Structures, Wind Tunnels, Wind Tunnel Technique. 130*s.* (post 3*s.* 3*d.*)

1946 Vol. I. Accidents, Aerodynamics, Aerofoils and Hydrofoils. 168*s.* (post 3*s.* 9*d.*)
Vol. II. Airscrews, Cabin Cooling, Chemical Hazards, Controls, Flames, Flutter, Helicopters, Instruments and Instrumentation, Interference, Jets, Miscellaneous, Parachutes. 168*s.* (post 3*s.* 3*d.*)
Vol. III. Performance, Propulsion, Seaplanes, Stability, Structures, Wind Tunnels. 168*s.* (post 3*s.* 6*d.*)

1947 Vol. I. Aerodynamics, Aerofoils, Aircraft. 168*s.* (post 3*s.* 9*d.*)
Vol. II. Airscrews and Rotors, Controls, Flutter, Materials, Miscellaneous, Parachutes, Propulsion, Seaplanes, Stability, Structures, Take-off and Landing. 168*s.* (post 3*s.* 9*d.*)

1948 Vol. I. Aerodynamics, Aerofoils, Aircraft, Airscrews, Controls, Flutter and Vibration, Helicopters, Instruments, Propulsion, Seaplane, Stability, Structures, Wind Tunnels. 130*s.* (post 3*s.* 3*d.*)
Vol. II. Aerodynamics, Aerofoils, Aircraft, Airscrews, Controls, Flutter and Vibration, Helicopters, Instruments, Propulsion, Seaplane, Stability, Structures, Wind Tunnels. 110*s.* (post 3*s.* 3*d.*)

Special Volumes

Vol. I. Aero and Hydrodynamics, Aerofoils, Controls, Flutter, Kites, Parachutes, Performance, Propulsion, Stability. 126*s.* (post 3*s.*)
Vol. II. Aero and Hydrodynamics, Aerofoils, Airscrews, Controls, Flutter, Materials, Miscellaneous, Parachutes, Propulsion, Stability, Structures. 147*s.* (post 3*s.*)
Vol. III. Aero and Hydrodynamics, Aerofoils, Airscrews, Controls, Flutter, Kites, Miscellaneous, Parachutes, Propulsion, Seaplanes, Stability, Structures, Test Equipment. 189*s.* (post 3*s.* 9*d.*)

Reviews of the Aeronautical Research Council

1939–48 3*s.* (post 6*d.*) 1949–54 5*s.* (post 5*d.*)

Index to all Reports and Memoranda published in the Annual Technical Reports

1909–1947 R. & M. 2600 (out of print)

Indexes to the Reports and Memoranda of the Aeronautical Research Council

Between Nos. 2351–2449	R. & M. No. 2450	2*s.* (post 3*d.*)
Between Nos. 2451–2549	R. & M. No. 2550	2*s.* 6*d.* (post 3*d.*)
Between Nos. 2551–2649	R. & M. No. 2650	2*s.* 6*d.* (post 3*d.*)
Between Nos. 2651–2749	R. & M. No. 2750	2*s.* 6*d.* (post 3*d.*)
Between Nos. 2751–2849	R. & M. No. 2850	2*s.* 6*d.* (post 3*d.*)
Between Nos. 2851–2949	R. & M. No. 2950	3*s.* (post 3*d.*)
Between Nos. 2951–3049	R. & M. No. 3050	3*s.* 6*d.* (post 3*d.*)
Between Nos. 3051–3149	R. & M. No. 3150	3*s.* 6*d.* (post 3*d.*)

HER MAJESTY'S STATIONERY OFFICE

from the addresses overleaf

Printed and published by
HER MAJESTY'S STATIONERY OFFICE

To be purchased from
York House, Kingsway, London W.C.2
423 Oxford Street, London W.1
13A Castle Street, Edinburgh 2
109 St. Mary Street, Cardiff
39 King Street, Manchester 2
50 Fairfax Street, Bristol 1
35 Smallbrook, Ringway, Birmingham 5
80 Chichester Street, Belfast 1
or through any bookseller

Printed in England

S.O. Code No. 23-3327